Univerzita Karlova v Praze

Přírodovědecká fakulta

Studijní program: Biologie

Studijní obor: Fyziologie živočichů

Bc. Denisa Koleničová

Úloha Wnt signalizační dráhy v proliferaci a diferenciaci neurálních kmenových buněk neonatálního a dospělého myšího mozku

The role of the Wnt signalling pathway in proliferation and differentiation of neural stem cells in the neonatal and adult mouse brain

Diplomová práce

Vedoucí diplomové práce: Ing. Miroslava Anděrová CSc.

Praha 2016

PROHLÁŠENÍ

Prohlašuji, že jsem závěrečnou práci zpracovala samostatně a že jsem uvedla všechny použité informační zdroje a literaturu.Tato práce ani její podstatná část nebyla předložena k získání jiného nebo stejného akademického titulu.

V Praze, 27.4.2016 .....

ACKNOWLEDGEMENTS

I would like to express my gratitude to my supervisor Ing. Miroslava Anděrová CSc. for the useful comments, remarks, listening to my ideas and problems and completing this thesis. Furthermore I would like to thank Mgr. Jan Kriška for his guidance during my experimental work.

Experimental work performed within thesis was funded by the grants GACR P303/12/0855 and GACR P304/12/G069 from the Grant Agency of the Czech Republic in the Department of Cellular Neurophysiology, Institute of Experimental Medicine, Academy of Science of the Czech Republic.

ABSTRACT

The canonical Wnt/β-catenin signalling pathway plays an important role in proliferation and differentiation of neural progenitors during embryogenesis as well as postnatally. In the present study, the effect of the Wnt signalling pathway on the differentiation potential of neonatal and adult neural stem cells (NS/PCs) isolated from subventricular zone (SVZ) of lateral ventricles and their membrane properties were studied eight days after the onset of *in vitro* differentiation. To manipulate Wnt signalling at different cellular levels, three transgenic mouse strains were used, which enabled inhibition or activation of the pathway using the Cre-loxP system. We showed that the activation of the Wnt signalling pathway leads to higher expression of β-catenin in both postnatal as well as adult NS/PCs, while Wnt signalling inhibition results in the opposite effect. To follow the fate of NS/PCs, the patch-clamp technique, immunocytochemistry, and Western blot were employed. After eight days of NS/PCs differentiation we identified three electrophysiologically and immunocytochemically distinct cell types of which incidence was significantly affected by the canonical Wnt signalling pathway, only in differentiated neonatal NS/PCs. Activation of this pathway suppressed gliogenesis, and promoted neurogenesis, while its inhibition led to the adverse effect. Surprisingly, manipulation of Wnt signalling in NS/PCs isolated from the SVZ of adult mouse brains had no effect on their differentiation potential. Therefore, the transgenic mouse strains used in this study represents suitable animal model for manipulating Wnt/β-catenin signalling in the SVZ of postnatal mouse brain.

Key words: Wnt/β-catenin signalling pathway, neonatal mice, adult mice, neural stem cells, neurogenesis, gliogenesis, patch-clamp technique

ABSTRAKT

Kanonická Wnt/β-katenin signální dráha hraje důležitou úlohu v proliferaci a diferenciaci neurálních progenitorů jak v průběhu embryogeneze, tak postnatálně. V této práci jsme se zaměřili na efekt Wnt signální dráhy na diferenciační potenciál neonatálních a dospělých neurálních kmenových buněk (NS/PCs) izolovaných ze subventrikulární zóny (SVZ) postranních komor myších mozků a jejich elektrofyziologické vlastnosti po osmi dnech *in vitro* diferenciace. Pro manipulaci Wnt signální dráhy na různých buněčných úrovních jsme použili tři transgenní myší kmeny, umožňující tamoxifenem indukovanou rekombinaci DNA, která vede k inhibici nebo aktivaci této dráhy. Ukázali jsme, že aktivace Wnt dráhy má za následek vyšší expresi β-kateninu u NS/PCs, zatímco její inhibice vede k opačnému účinku. K charakterizaci diferencovaných NS/PCs bylo využito metody terčíkového zámku, imunocytochemického barvení a Western blotu. Po osmi dnech differenciace NS/PCs jsme identifikovali tři elektrofyziologicky a imunocytochemicky rozdílné buněčné typy jejichž incidence je do značné míry ovlivněna kanonickou Wnt signální dráhou, pouze u NS/PCs. Aktivace již zmíněné dráhy potlačila gliogenezi, ale podpořila neurogenezi, zatímco její inhibice vedla k opačnému efektu, tedy k potlačení neurogeneze a podpoře gliogeneze. Prekvapivě, manipulace Wnt signální dráhy neměla žádný dopad na diferenciační potenciál dospělých NS/PCs. Z toho důvodu transgenní myší kmeny, použité v této studii, mohou sloužit jako vhodné zvířecí modely pro manipulaci Wnt/β-katenin signální dráhy pouze v neonatálním myším mozku.

Klíčová slova: Wnt/β-katenin signální dráha, neonatální myši, dospělé myši, neurální kmenové buňky, neurogeneze, gliogeneze, metoda terčíkového zámku

LIST OF ABBREVIATIONS

4-OHT= 4-hydroxytamoxifen

3-PGDH= 3-phosphoglycerate dehydrogenase

β III tubulin= β-tubulin isotype III

β-CAT= β-catenin

pβ-CAT= phosphorylated β-catenin

β-TrCP= β-transducing-containing protein

ALDH1L1= aldehyde dehydrogenase 1 family member L1

APC= adenomatous polyposis coli

ARM= armadillo repeats

B1 domains= domains of B1-cells

bFGF= basic fibroblast growth factor

BMPs= bone morphogenetic proteins

BV= blood vessels

CA= *cornu Ammonis*

CaMKII= calmodulin dependent protein kinase II

Cm= membrane capacitance

cGMP= cyclic guanosine monophopshate

CNS= central nervous system

Cre= Cre recombinase

CreERT2= Cre recombinase/modified form of the estrogen receptor

CTD= C-terminal domains

CTRL= control

DAPI= 4',6-diamidino-2-phenylindole

DCX= doublecortin

DG= dentate gyrus

Dkks= Dickkopf proteins

DNA= deoxyribonucleic acid

dn-TCF4= dominant negative T-cell factor

Dvl= Dishevelled protein

E2-E10= exon 2-10

EGFP= enhanced green fluorescent protein

FGFs= fibroblast growth factors

Fzd= Frizzeld

GAD65= glutamate decarboxylase 65

GAM/GAR 488/594/660= goat anti-mouse/rabbit IgG conjugated with Alexa Fluor 488/594/660

GCL= granule cell layer

GCs= granule cells

GFAP= glial fibrillary acidic protein

GFAP-Cy3= glial fibrillary acidic protein coupled with the Cy3 fluorescent dye

GL= glomerular layer

GS= glutamate synthetase

GSK3β= glycogen synthase kinase 3β

hA= horizontal astrocytes

HRP= horseradish peroxidase

ICAT= inhibitor of β-catenin

ICC= immunohistochemistry

IGCs= immature granule cells

IML= inner molecular layer

IP3= inositol triphosphate

IPCs= immature progenitors

JNK= Jun-N-terminal kinase

K_A= fast activating and inactivating outwardly rectifying K^+ currents

K_{DR}= delayed outwardly rectifying K^+ current

K_{IR}= = inwardly rectifying K^+ currents

L1= long interspersed element-1

LEF= lymphoid enhancer-binding factor

LRP5/6= lipoprotein receptor-related proteins 5 and 6

LV= lateral ventricles

MAPs= microtubule associated proteins

MBP= myelin basic protein

mRNA= messenger RNA

Msi1= Musashi1

NeuroD1= neurogenic differentiation1

NeunN= neuronal specific nuclear protein

NG2= neural antigen 2

Non-pβ-catenin= non-phosphorylated β-catenin

NS/PCs= neural stem/progenitor cells

NSCs= neural stem cells

NTD= N-terminal domains

OB= olfactory bulb

OPCs= oligodendrocyte precursor cells

pβ-CAT= phosphorylated β-catenin

pA= polyadenylation site

PB= phosphate buffer

PBS= phosphate-buffered saline

PAGE= polyacrylamide gel electrophoresis

PCP= planar cell polarity

PDGFαR= platelet-derived growth – factor-α-receptor

PGK-Neo= neomycin resistance casette

PLC= phospholipase C

PKC= protein kinase C

PLP = proteolipid protein 1

Prox1= prospero homeobox protein1

PSA-NCAM= polysialyted-neural cell adhesion molecule

rA= radial astrocytes

RA domains= domains of radial astrocytes

RMS= rostral migratory stream

RNA= ribonucleic acid

ROCK= Rho-associated protein kinase

ROS= random regions of interest

RT-qPCR= quantitative reverse-trancription polymerase chain reaction

S100β= calcium binding protein

sFRPs= secreted Fzd related proteins

SGZ= subgranular zone

SHH= sonic hedgehog homolog

Sox2= SRY (sex determining region Y)-box 2

SVZ= subventricular zone

TCF= T-cell specific transcription factor

TCF4= transcription factor4

TTX= tetrodotoxine

TUC-4= protein related to axonal outgrowth

TUJ1= class III β-tubulin

Vm= membrane potential

VZ= ventricular zone

WB= western blot

WIF1= Wnt inhibitory factor 1

Wnt= Wingless/Integrated

TABLE OF CONTENTS

INTRODUCTION

Even at the beginning of the 20th century scientists were convinced, that the central nervous system (CNS) has no ability to regenerate. However, this paradigm was broken in 1965, when authors Altman and Das published an article entitled *"Autoradiographic and histological evidence of postnatal neurogenesis in rats"*. In this study, they demonstrated the existence of cell proliferation in the adult rat brain. In 1998, thirty-three years later, Ericson and colleagues discovered a generation of new neurons also in the human brain. These discoveries influenced, to a large extent, the current direction of the research, when the laboratories all over the world are examining the potential of neural stem/progenitor cells (NS/PCs).

The Wnt signalling pathway is implicated in many cell processes, such as cell patterning, proliferation, differentiation or programmed cell death and *in vitro* studies on newborn mice have suggested that the Wnt signalling pathway has also an effect on proliferation and differentiation of NS/PCs. Three major Wnt signalling pathways have been characterized: canonical Wnt/β-catenin signalling pathway and two non-canonical signalling pathways, which are all activated by binding Wnt protein to a receptor from the Frizzled (Fzd) family. The canonical Wnt signalling pathway is dependent on the molecule β-catenin, which plays a crucial role in gene transcription and cell adhesion.

The aim of the present study was to elucidate the role of the Wnt/β-catenin signalling pathway in the neurogenesis and gliogenesis of NS/PCs isolated from subventricular zone (SVZ) of lateral ventricles of neonatal and adul mouse brains. To identify the differentiation potential of neonatal and adult NS/PCs, we studied their membrane properties eight days after the onset of *in vitro* differentiation. To manipulate Wnt signalling at different cellular levels, three transgenic mouse strains were used, which enabled inhibition or activation of the pathway using the tamoxifen-inducible Cre-loxP system. The phenotype of differentiated cells was analysed using the patch-clamp technique, immunocytochemical staining, and Western blot analysis.

1 LITERATURE REVIEW

1.1 Embryonic stages of neurogenesis and gliogenesis

In the developing CNS all neurons and macroglia are derived from neuroepithelial cells that line the cerebral ventricles and the spinal canal (Figure 1A). At embryonic days (E9 and E10), progressive waves of neurogenesis begin at caudal regions of the spinal cord and proceed rostrally, to the mouse brain. In the embryonic neurogenesis, radial glia cells represent primary progenitor cells, they line the forebrain ventricles and the spinal canal, maintain apical-basal polarity, and undergo migration in association with cell-cycle progression (Miyata et al., 2001).

In general, glial cells are generated after neurogenesis and guide neuronal migration, but radial glia are an exception to this rule (Noctor et al., 2004). They are generated before neurogenesis and guide newly derived neurons (Rakic, 1972). These cells are mitotically active throughout neurogenesis and become astrocytes when the neuronal migration is completed (Figure 1A) (Misson et al., 1988). Oligodendrocyte precursors and ependymal cells are also derived from radial glia (Figure 1B), but whether intermediate progenitors are involved remains unresolved. Intermediate progenitors are the main proliferative cells of the SVZ of the embryonic telencephalon and seem to be restricted to producing neurons or glia (Figure 1C) (Noctor et al., 2004).

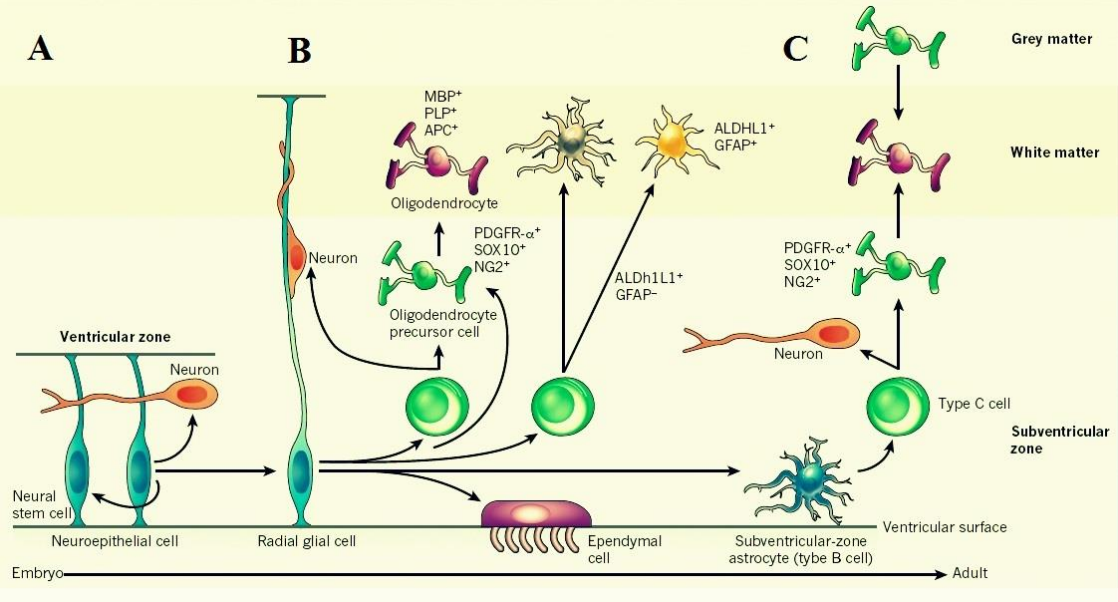

Figure 1: Gliogenesis from embryo to adult. From the left to the right: the development of neuronal cells from the embryo to the adult. **A:** Neurogenesis starts, when neuroepithelial cells are transformed into radial

glia. A few of neuroepithelial cells generate also some neurons. **B:** Radial glia cells can produce intermediate progenitor cells or OPCs, which in turn produce neurons and oligodendrocytes. Radial glia cells generate also astrocytes and ependymal cells. **C**: In the adult mouse brain oligodendrocytes are produced by two independent pathways. The first pathway takes place in the subventricular zone, where B-cells give rise to C-cells, also known as transit amplifying cells. These cells in turn produce OPCs as well as neurons. The OPCs subsequently generate oligodendrocytes. The second pathway is through OPCs in the grey matter. These cells also produce oligodendrocytes. **Abbreviations: ALDH1L1**= aldehyde dehydrogenase 1 family member L1; **APC**= adenomatous polyposis coli; **GFAP**= glial fibrillary acidic protein; **MBP** = myelin basic protein, OPCs= oligodendrocyte precursor cells; **PDGFαR**= platelet-derived growth – factor-α- receptor; **PLP**= proteolipid protein 1 (Rowitch and Kriegstein, 2010).

The *in vivo* potential of neuroepithelial cells and radial glia becomes regionally restricted thorough the action of organizing signals such as fibroblast growth factors (FGFs), Sonic hedgehog (SHH), WNTs and bone morphogenetic proteins (BMPs). All of these signals provide positional information through morphogen gradients in the dorso- ventral, anterio-posterior, and medio-lateral axes (Briscoe and Novitch, 2008).

1.2 Neurogenesis and gliogenesis in the adult mouse brain

In the postnatal as well as adult brains of mammals, including humans, NS/PCs are generated in two neurogenic regions: the dentate gyrus (DG) of the hippocampus and SVZ (Figure 2) (Altman and Das, 1965).

The hippocampus is localized in the medial temporal lobe. Together with the amygdala, cingulate cortex and olfactory cortex, the hippocampus belongs to the limbic system. This brain region plays important roles in the consolidation of information from short-term memory to long-term memory and spatial navigation. In addition, more than 250 000 new neurons are incorporated in the rodent DG every month (Cameron and McKay, 2001), namely in the subgranular zone (SGZ) of DG.

Another region, where neurogenesis was found in the adult brain, is the SVZ. It is a paired brain structure situated throughout the lateral walls of the lateral ventricles (LV) (Figure 3A). It is interesting that SVZ is composed of four different layers (layer I, layer II, layer III and layer IV), which are distinct in many parameters such as thickness, cell density or also cellular composition. While layer I is a monolayer of ependymal cells, layer II and III contain predominantly astrocytes. Layer IV is considered to represent a transition zone between layer III and the parenchyma of the brain.

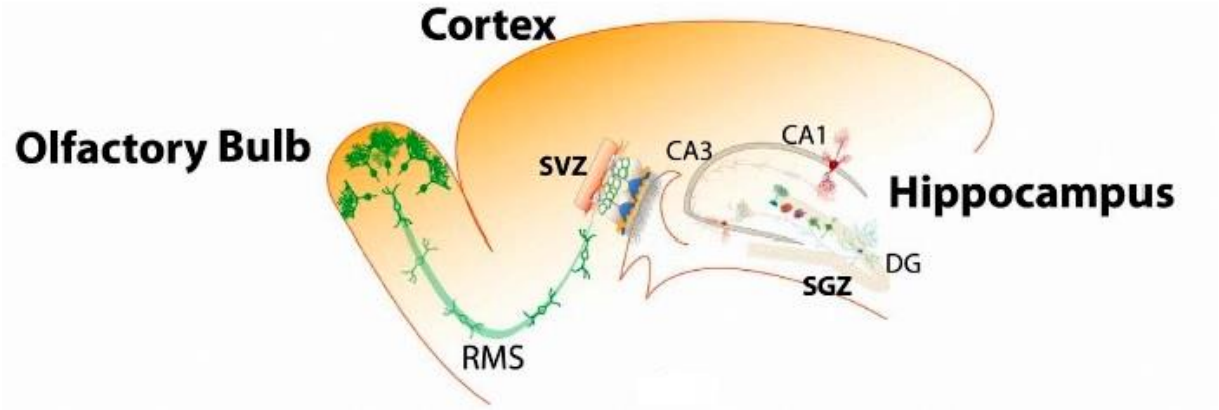

Figure 2: Neurogenic regions in the adult brain. Schematic illustration of two neurogenic regions: the hippocampus and the SVZ. Three parts of the hippocampus: CA1, CA3 and the DG. Neurogenesis lingers in the SGZ of the DG in the adult brain. **Abbreviations: CA=** cornu Ammonis; **DG**= dentate gyrus; **RMS**= rostral migratory stream; **SGZ**= subgranular zone; **SVZ**= subventricular zone (Varela-Nallar and Inestrosa, 2013).

1.2.1 The cell architecture of subventricular zone

The architecture of the adult SVZ is well characterized at the ultrastructural level. In the mouse adult SVZ four types of cells were characterized (Figure 3B):

a) **Neuroblasts**: also known as A-cells, which migrate as homotypic chains (Doetsch, 2003).
b) **Astrocytes**: also known as B1-cells that are derived from radial glia. They often form clusters with one another. (Mirzadeh et al., 2008).
c) **Transit amplifying cells**: or C-cells are dispersed along the network of chains (Doetsch, 2003).
d) **Ependymal cells:** also known as E-cells. In the SVZ two types of ependymal cells, E1 and E2-cells are located. E1-cells represent multiciliated ependymal cells. E2 cells are ultrastructurally similar to E1-cells but E2-cells are characterized by only two cilia and extraordinarily complex basal bodies. The most characteristic attribute of E2-cells is their large basal bodies (Mirzadeh et al., 2008).

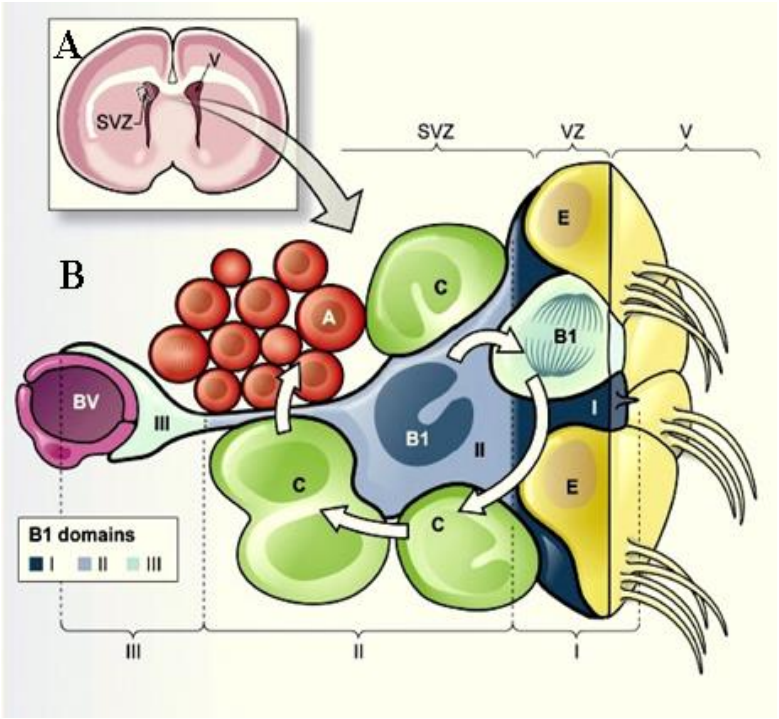

Figure 3: Cellular composition in the subventricular zone. A: The location of the SVZ in the adult mouse brain. **B:** The cellular composition of the adult SVZ. In this region of the brain four types of cells are located. Neural stem cells also known as B1-cells (blue), multicilliated ependymal cells or E-cells (yellow), intermediate progenitors also known as C-cells or transit amplifying cells (green). **Abbreviations: B1 domains**= domains of B1-cells; **BV**= blood vessels; **LV**= lateral ventricle; **SVZ**= subventricular zone; **VZ**= ventricular zone (Fuentealba et al., 2012).

B1-cells are neural stem cells (NSCs) (Doetsch et al., 1999), however they are morphologically similar to non-neurogenic astrocytes in other regions and they also express glial fibrillary acidic protein (GFAP) (Figure 4C). These cells proliferate slowly and permanently and they give rise to C-cells. C-cells, also known as "transit amplifying cells" (Figure 4A), proliferate quickly and they become neuroblasts (Doetsch et al., 1999). The Wnt/β-catenin signalling pathway is the regulator of the proliferation and differentiation of the C-cells and by increasing the proliferation of C-cells, it also increases their pool, which eventually leads to an increase in number of newly generated neurons in the olfactory bulb (OB) (Adachi et al., 2007). C-cells generate A-cells (neuroblasts), which migrate into the OB, the anterior tip of the telencephalon (Figure 4B). It is also important that A-cells migrate into the OB through the rostral migratory stream (RMS) (Kaneko and Sawamoto, 2009).

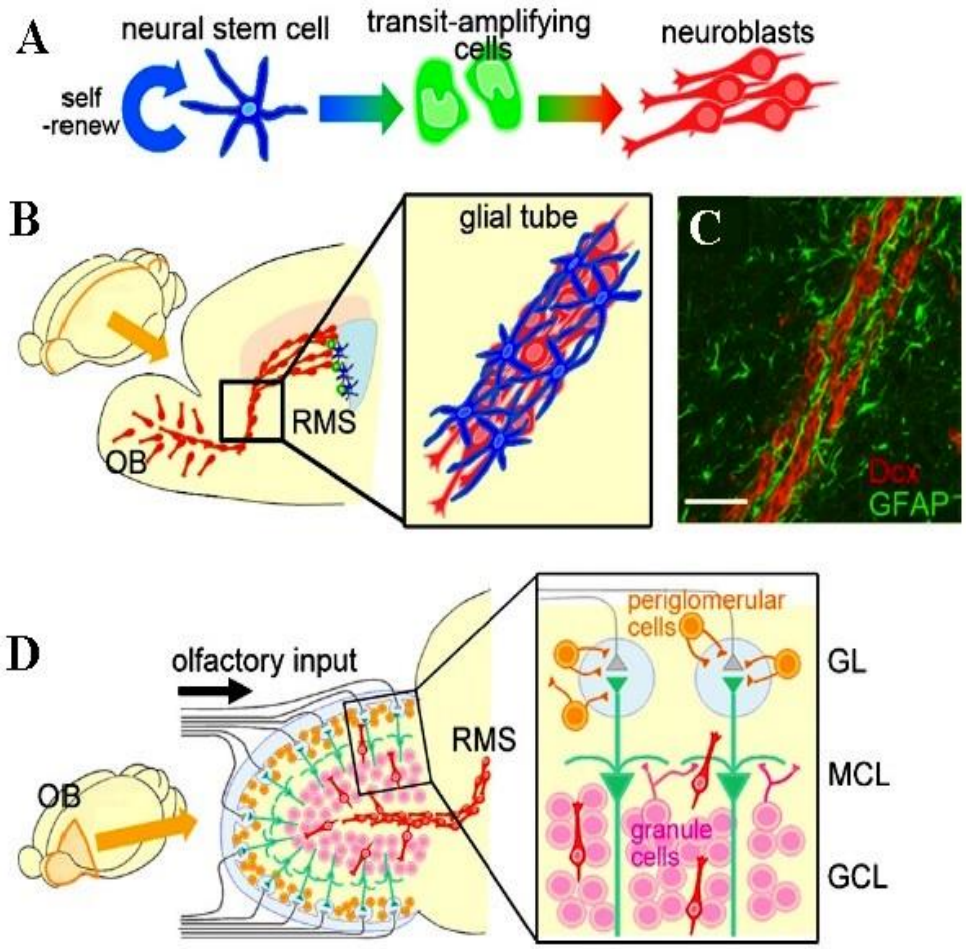

Figure 4: Production of new neurons of the subventricular zone A: astrocytes or neural stem cells (blue) in the SVZ generate transit amplifying cells (green). These cells proliferate quickly and produce neuroblasts (red). **B:** Newly born neuroblasts migrate into the OB through RMS that is formed by neuroblasts (red chain-like clusters) surrounded by a so-called glial tube (blue astrocytic sheath). **C:** Immunohistochemistry against DCX and GFAP **D:** Neuroblasts in the OB differentiate into two types of olfactory interneurons, granule cells or periglomerular cells, which reside in the GCL or GL. **Abbreviations: DCX=** doublecortin; **GCL**=granular cell layer; **GFAP**= glial fibrillary acidic protein; **GL**= glomerular layer; **OB**= olfactory bulb; **SVZ**= sunventricular zone; **RMS**= rostral migratory stream (Kaneko and Sawamoto, 2009).

A-cells generated in the SVZ during neurogenesis migrate along the RMS at high speed (~100μm/h) for a distance about 5 mm. In the RMS they form chain-like clusters that are surrounded by an astrocytic sheath called the glial tube (Kaneko and Sawamoto, 2009). Sawamoto and colleagues showed that the migration of A-cells along the RMS is in parallel with directional flow of cerebrospinal fluid in the LV. The gradient of diffusible proteins is caused by the cerebrospinal fluid from the choroid plexus in the LV. One of

these proteins is called Slit-protein. It helps A-cells migrate into the OB (Sawamoto et al., 2006). In the OB are chains of A-cells separated and further migrate independently, either into the granule cell layer (GCL) or glomerular layer (GL). A-cells, which migrated into the GCL generate granular interneurons, while those migrating into the GL differentiate into periglomerular cells (Figure 4D) (Merkle et al., 2007).

1.2.2 The cell architecture of the hippocampus

The hippocampus is composed of three distinct parts: *cornu Ammonis* (CA), which has another subdivision into CA1-CA4, subiculum and DG (Figure 5A). Adult neurogenesis (in the mammals) takes place only in the SGZ of the DG of the hippocampus (Figure 5B). The SGZ is a narrow layer of cells located between the granule cell layer and the *hilus* of the DG. In SGZ there are two populations of astrocytes, radial and horizontal astrocytes (Seri et al., 2001), which are different in many aspects.

Horizontal astrocytes are elongated but radial astrocytes have a round, polygonal or triangular cell body. For both types of astrocytes it is typical that they have light cytoplasm, a dense network of intermediate filaments, chromatin in granules, thin Golgi apparatus, mitochondria darker than neurons, small endoplasmic reticulum, and very importantly, they are in contact with other astrocytes through gap junctions. For radial astrocytes it is characteristic that they have more organelles, polyribosomes, and lighter mitochondria compared to horizontal astrocytes (Seri et al., 2004)

Some differences can be also found in immunocytochemical characteristics. A dominant difference is that nestin, a marker of neuroepithelial stem cells is present in radial astrocytes, but not in horizontal astrocytes. In contrast, horizontal astrocytes, but not radial astrocytes, stain with a β-subunit of calcium binding protein, S100β (Cocchia et al., 1981). Both types of astrocytes stain with GFAP, a marker of "mature" astrocytes (Bignami and Dahl, 1973), vimentin, a marker of "immature" astrocytes (Sancho-Tello et al., 1995), Musashi1 (Msi1), an RNA binding protein specific to astrocytes (Sakakibara et al., 1996) and 3-phosphoglycerate dehydrogenase (3-PGDH), an enzyme unique to radial glia, astrocytes, and neuroepithelial cells (Yamasaki et al., 2001).

Radial astrocytes are probably primary progenitors. They generate C-cells, which progressively differentiate into immature granule cells, which subsequently give rise to mature granule cells (GCs) (Figure 5C).

In 2007, Suh and colleagues identified a population of Sox^{2+} cells, which have the potential to differentiate into neurons and astrocytes in the SGZ. A marker of these cells is the Sex-determining Region Y (SRY)-related transcription factor. It is expressed during development in neural epithelial cells and embryonic stem cells. Two types of Sox^{2+} cells were identified in the SGZ: radial and non-radial cells based on their morphology. Both types of these cells, presumably represent NS/PCs. Division of radial stem cells is asymmetric, giving rise to one non-radial cell and one DCX^{+} precursor, which may subsequently generate new neurons. This model is very attractive, because NS/PCs can be capable of self-renewing and also generating new neurons at the same time (Suh et al., 2007)

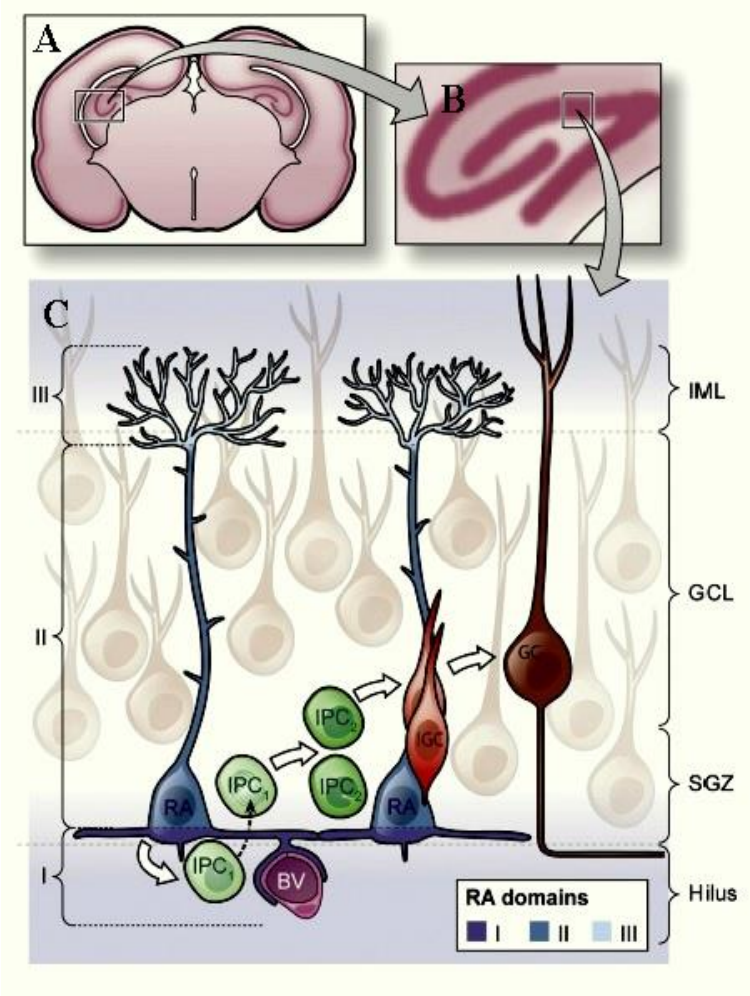

Figure 5: Cellular composition of the subgranular zone. The schematic illustration shows different domains of RA in SGZ. **A:** The hippocampal formation. **B**: The location of the DG of the hippocampus. **C:** The cellular composition of the DG. RA (blue) give rise to IPCs, also known as C-cells or transit amplifying cells. These cells gradually (via IPC_1 and IPC_2; green) differentiate into immature IGC (red). IGCs give rise to mature GCs (brown). **Abbreviations: BV**=blood vessels**; DG=** dentate gyrus; **GCs**= granule cells; **GCL**= granular cell layer; **IGCs**= immature granule cells; **IML**=inner molecular layer; **IPCs**= intermediate progenitor cells; **RA domains**= domains of radial astrocytes; **SGZ**= subgranular zone (Fuentealba et al., 2012).

In 2001 Seri and colleagues identified D-cells as intermediate precursors of new granule neurons in the DG. They are generated from radial astrocytes. In comparison with radial and horizontal astrocytes, D-cells have a very different ultrastructure, such as smooth plasma membrane, dark cytoplasm, many polyribosomes, mitochondria lighter than those

of astrocytes, and the endoplasmic reticulum larger than astrocytes, but smaller than mature granule neurons are typical for these cells (Seri et al., 2001).

D-cells generally make clusters of two or four cells. Markers of D-cells are doublecortin (DCX), a protein related to axonal outgrowth (TUC-4) and a polysialylated-neural cell adhesion molecule (PSA-NCAM). D-cells are also stained positively for neurogenic differentiation 1 (NeuroD1), a transcription factor, which regulates neuronal differentiation and prospero homeobox protein1 (Prox1), a homeobox gene expressed in dentate GCs in the postnatal brain. According to the results from confocal and electron microscopy D1, D2 and D3cells were characterized (Seri et al., 2004):

a) **D1-cells**: are round or have shape of an inverted drop.

b) **D2-cells**: have a short thick process that sometimes bifurcates. Three other subtypes of D2-cells were defined according to the orientation of their process: D2v, D2h and D2i-cells. D2v-cells have their process oriented vertically within the GCL. D2h-cells have the process horizontally, parallel to the blades of the DG. D2i-cells have the process inverted away from the GCL and pointing towards the hilus.

c) **D3-cells**: possess the characteristics of immature neurons. Usually they are found in the interference of the GCL and the SGZ (Seri et al., 2004).

D1-cells generate D2-cells. D2-cells give rise to D3-cells, which mature into new granule neurons. D-cells create clusters. As cells mature, they transfer into the GCL to reside next to matured granule neurons (Seri et al., 2004).

The local circuitry of the DG comprises excitatory neurons and inhibitory interneurons that participate in the networks behaviour. Granule cells in the DG project to the CA3 region, which, in addition to a robust recurrent connection, project to the CA1 region. The CA1 then projects back to the entorhinal cortex and subiculum regions, closing “the hippocampal loop” (Figure 6) (Aimone et al., 2014).

Between mature and immature neurons there are not only structural but also physiological differences. Immature neurons have a high input resistance, exhibit much greater synaptic plasticity and receive less inhibition (Aimone et al., 2014).

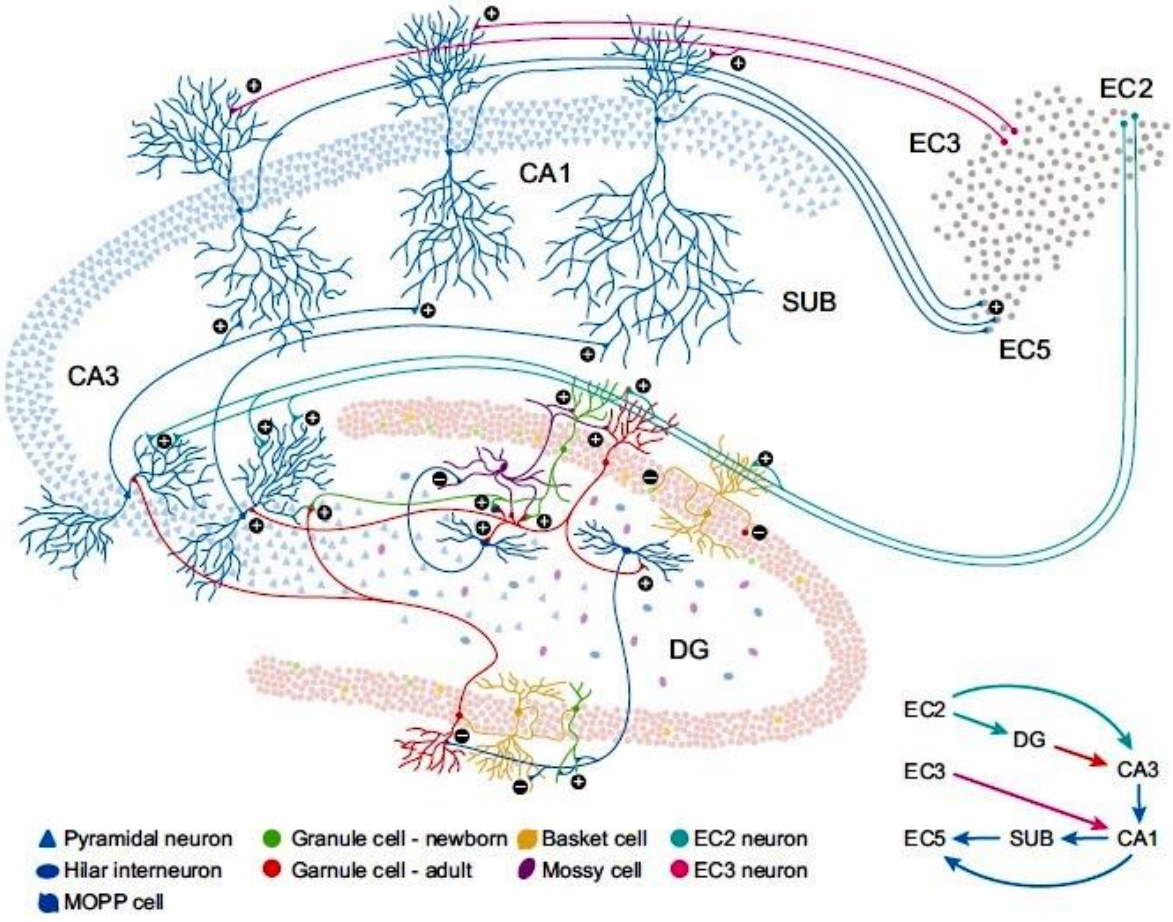

Figure 6: Integration of new neurons in the dentate gyrus of the hippocampus. The circuitry of the DG is characteristic by its complexity. The networks behaviour is influenced by inhibitory and excitatory neurons (mossy cells). GCs in the DG protrude to the CA3 region an then to the CA1 region which project back to the entorhinal cortex and the subiculum. **Abbreviations: CA=** cornu Ammonis; **DG=** dentate gyrus; **GCs=** granule cells (Aimone et al., 2014).

1.3 The Wnt signalling pathway

Wnt signalling pathway has many important functions in the organism. After discovering its function in carcinogenesis, it was documented, that the pathway has a very important role in the embryonic development. In the CNS, it has been related to several processes as synaptogenesis (Rosso and Inestrosa, 2013), mitochondrial dynamics, inflammation (Cisternas et al., 2014), neurogenesis and regeneration (Varela-Nallar and Inestrosa, 2013). Deregulation of the Wnt signalling pathway has been connected with diseases such as diabetes, schizophrenia, Parkinson´s and Alzheimer´s disease.

Three major Wnt signalling pathways have been identified: the canonical Wnt /β-catenin pathway and two non-canonical pathways – Wnt/PCP and the Wnt/Ca^{2+} pathway. All three

pathways are activated after the binding of the Wnt ligand to a receptor from the Frizzled family.

1.3.1 The canonical Wnt signalling pathway

The canonical Wnt signalling pathway is dependent on the β-catenin. This protein consists of a central region made up of 12 Armadillo (ARM) repeats that are flanked by distinct N-terminal domains (NTD) and C-terminal domains (CTD). A specific conserved helix (Helix C) is located proximally to the CTD, adjacent to the last ARM repeat. The NTD and the CTD may by structurally flexible, whereas the central region forms a relatively rigid scaffold (Huber et al., 1997).

In the cell β-catenin has many various functions. For example, it is the integral structural component of cadherin-based adherens junction (Ozawa et al., 1989), it activates the T-cell specific transcription factor (TCF)/ the lymphoid enhancer-binding factor (LEF) family of transcription factors (Huber et al., 1996), and it is involved in the amplification and separation of centrosomes. The biochemical analyses revealed that many of β-catenin binding partners share overlapping binding sites in the groove of the central β-catenin region: consequently, these partners cannot bind to β-catenin simultaneously. This mutual exclusivity is certainly valid for the key β-catenin interacting molecules:

a) **E-cadherin**: the main partner in adherens junction.
b) **Adenomatous polyposis coli** (APC): the main partner in the destruction complex.
c) **TCF/LEF:** the main partner in the nucleus (Graham et al., 2000).

The key element of canonical Wnt signalling, β-catenin plays a crucial role in gene transcription and cell adhesion (Mosimann et al., 2009). In this pathway, the interaction between a Wnt ligand and its receptor Frizzled (Fzd), triggers the recruitment of Axin to the plasma membrane, resulting in the inhibition of β-catenin phosphorylation by glycogen synthase kinase 3β (GSK-3β) and the subsequent escape from degradation in the proteasome. The protein thus accumulates in the cytoplasm and then trans-locate into the nucleus, where it forms a complex with transcription factors; TCF/LEF, which leads to the activation of target genes (Figure 7A) (Städeli et al., 2006).

In the absence of Wnt stimulation, the destruction complex is formed in the cytoplasm. The destruction complex comprises of the scaffold proteins Axin, APC, casein kinase I, and the enzym GSK3β an its role is the phosphorylation of the β-catenin in the cytoplasm (Ikeda et

al., 1998). The phosphorylated β-catenin binds with the β-transducing-containing protein (β-TrCP) and then is degraded in the proteosome (Liu et al., 2002). The Wnt signalling pathway can be inhibited by:

a) **Dickkopf proteins** (Dkks): represent a small family of glycoproteins, which can be found in invertebrates, such as *Dictiostelium*, urochordates, cnidarians, ascidians, but also in vertebrates, including humans. In vertebrates the Dkk family comprises four proteins: Dkk1, Dkk2, Dkk3, and Dkk4. Dkks can specifically inhibit the Wnt/β-catenin pathway by binding to the LRP 5/6 (Cruciat and Niehrs, 2013).

b) **Secreted Fzd related proteins** (sFRPs): represent the largest family of Wnt inhibitors, which can be found in invertebrates (but not in *Drosophila*), and also in vertebrates. There are five types of Fzd related proteins in humans: sFRP1, sFRP2, sFRP3, sFRP4, and sFRP5 (Bovolenta et al., 2008). Many studies indicate that sFRPs are not only Wnt binding proteins, but they can also bind to the Fzd receptors and provide axon guidance information (Rodriguez et al., 2005).

c) **Wnt inhibitory factor 1** (WIF1): was for the first time identified as an expressed sequence tag from the human retina. Moreover, WIF1 can be found in a variety of tissues, because is expressed not only in the retina, but also in the brain, the cartilage, and the lungs (Hsieh et al., 1999). The mechanism of regulation of the Wnt signalling pathway by WIF1 is not completely understood.

d) **Inhibitor of β-catenin** (ICAT): and T-cell factor4 (TCF4) can inhibit the Wnt signalling pathway in the nucleus. This inhibitor antagonises Wnt signalling by preventing the complex formation between β-catenin and TCF4 (Tago et al., 2000).

1.3.2 The non-canonical Wnt signalling pathway

The non-canonical Wnt signalling pathway comprises two basic intracellular cascades: the Wnt/PCP and the Wnt/Ca^{2+} pathway.

a) **The Wnt/planar cell polarity signalling pathway**: the activation of this signalling pathway leads to the activation of small GTP-ase proteins, Rho and Rac and consequently to the activation of Rho-associated protein kinase (ROCK) and Jun-N-terminal kinase (JNK). Jun-N-terminal kinases can translocate into the nucleus and they regulate expression of genes or modify the cytoskeleton stability as they

affect the phosphorylation of microtubule-associated proteins (MAPs) and interact with actin-regulator proteins (Figure 7C) (Axelrod et al., 1998).

b) **The Wnt/Ca^{2+} signalling pathway:** triggers the activation of trimeric G-protein and phospholipase C (PLC), that increases the production of inositol triphosphate (IP3). Inositol triphosphate increases the concentration of intracellular Ca^{2+} and decreases the levels of cyclic guanosine monophosphate (cGMP). The intracellular aggrandisement of Ca^{2+} activates protein kinase C (PKC) and calmodulin-dependent protein kinase II (CaMKII). These kinases can stimulate different transcription factors, for example, nuclear factor of activated T-cells (Figure 7B) (Kühl et al., 2000).

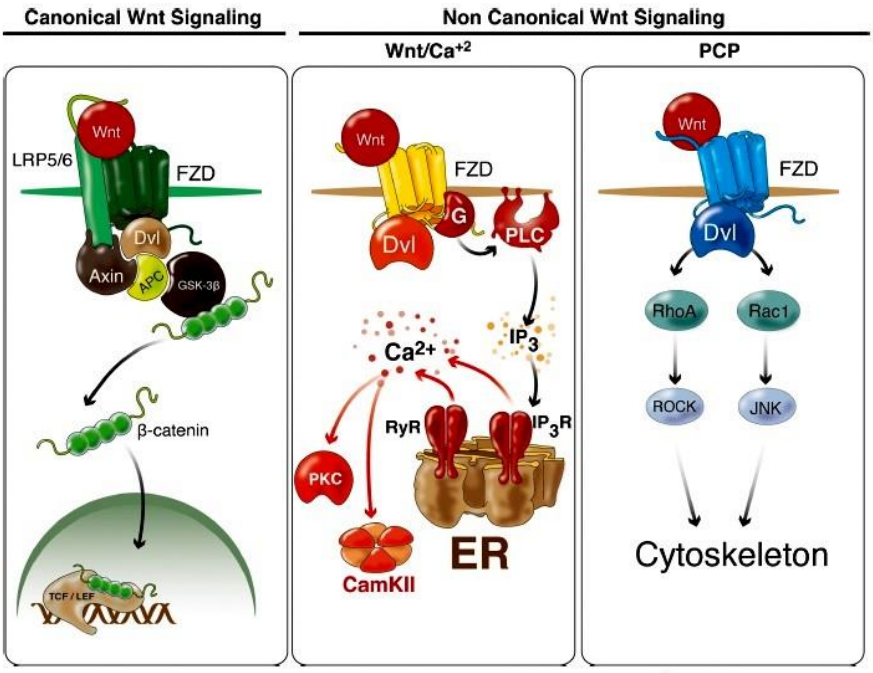

Figure 7: Canonical and non-canonical Wnt signalling pathways. A) The canonical Wnt/β-catenin signalling pathway: the Wnt protein binds to the Fzd receptor and to the LRP5/6, which serve as a coreceptor for Wnt ligands. Fzd receptor interacts with Dvl. Activation of Dvl inhibits GSK3β. This process leads to accumulation of β-catenin in the cytoplasm and its translocation into the nucleus. **B) Non-canonical Wnt/calcium signalling pathway (Wnt/Ca^{2+})**: the activation of this signalling pathway initiates the activation of trimeric G-protein and PLC increasing IP3 Subsequently IP3 induces the release Ca^{2+} from the ER. **C) Non canonical Wnt/planar cell polarity signalling pathway:** activation of the cascade triggers the activation of small GTPases Rho and Rac. This results in the activation of ROCK and JNK to regulate cytoskeleton dynamics**. Abbreviations: CAMK II=** calmodulin-dependent protein kinase; **Dvl=** Disheveled; **Fzd=** Frizzled; **GSK3β**= glycogen synthase kinase 3β; **IP3**= inositol triphosphate; **JNK**= JUN N-terminal

kinase; **LEF**= lymphoid enhancer factor; **LRP 5/6**= low-density lipoprotein receptor-related protein 5/6; **PCP**= planar cell polarity; **TCF**= T-cell factor; **PLC**= phospholipase C; **ROCK**= Rho-associated protein kinase; **Wnt**= Wingless/Integrated (Inestrosa and Varela-Nallar, 2015).

1.4 The role of the Wnt signalling pathway in neurogenesis

Many signalling cascades are involved in the regulation of the different steps of neurogenesis and they are responsible for the proper balance between the maintenance of the neural stem cells pool and for differentiation an maturation of newborn neurons. In recent years, increasing evidence support a role of the Wnt/β-catenin pathways in the regulation of neonatal and adult neurogenesis. Until now: nineteen members of the Wnt family and 10 members of the Fzd family have been indentified in mammals:

a) **Wnt3**: is a protein that is encoded in humans by the *WNT3* gene. Using in situ hybridization Lie and colleagues showed that Wnt3 protein is expressed in close proximity to the SGZ, which is important for proliferation and differentiation of adult hippocampal stem cells into granule neurons. Moreover overexpression of Wnt3 protein is sufficient to increase neurogenesis from adult hippocampal stem cells *in vitro* and *in vivo*. Conversely, blockade of Wnt signalling pathway reduces neurogenesis from adult stem cells *in vitro* and abolishes neurogenesis almost completely *in vivo*. These data suggest that Wnt signalling pathway is a principal regulator of adult hippocampal neurogenesis and provide evidence that Wnt proteins have a key role in adult hippocampal function (Lie et al., 2005).

b) **Wnt5**: regulates axonal behavior in symphatetic and cortical neurons. In cortical neurons this protein stimulates axonal outgrowth and repulsive axon guidance through different receptors. The axonal outgrowth is mediated by the Ryk receptor, but axonal repulsion requires both Ryk and Fzd receptors (Li et al., 2009).

c) **Wnt7b**: regulates dendritic arborization. This effect is mediated by the noncanonical Wnt signalling cascade, which involves activation of JNK (Rosso et al., 2005).

d) **Fzd5**: regulates a very early event in neuronal development, establishment of neuronal polarity. Overexpression of FZD5 induces a loss of polarized receptor distribution and mislocalization of axonal proteins, while Fzd5 knockdown induces a loss of axonal proteins (Figure 8) (Slater et al., 2013).

e) **Beta-catenin:** in hippocampal neurons is a critical mediator of dendritic morphogenesis. This function of β-catenin is independent of gene transcription and it is required for dendritic growth induced by depolarization (Yu and Malenka, 2003). Recently, increasing evidence has supported a role for the Wnt/β-catenin signalling pathways in the regulation of adult neurogenesis

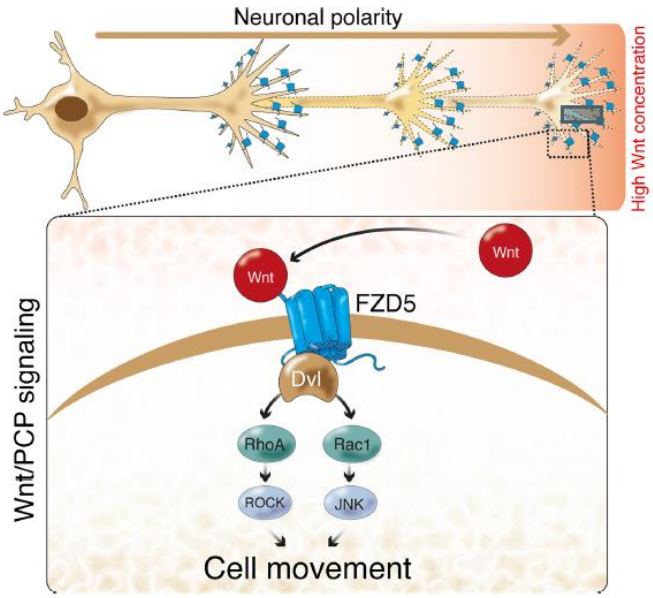

Figure 8: The role of Fzd5 receptor in neuronal polarity and morphogenesis. The protein Fzd5 is located in the peripheral zone of axonal growth cones. Gain and loss of function experiments demonstrate that Fzd5 has an important role in neuronal polarity. Overexpression of Fzd5 in neurons that are already polarized decrease the total length of axons, a process partially prevented by inhibition of JNK, which suggests that the Wnt/PCP patway modulates axon behavior. **Abbreviations: Dvl=** Disheveled; **Fzd=** Frizzled; **JNK**= JUN N-terminak kinase; **PCP**= planar cell polarity **ROCK**= Rho associated protein kinase; **Wnt**= Wingless/Integrated (Inestrosa and Varela-Nallar, 2015).

How it is possible, that the Wnt/β-catenin signalling pathway could regulate neurogenesis:

a) **Neurogenic differentiation 1** (NeuroD1): is a transcription factor, belonging to a part of NeuroD family of basic helix-loop-helix transcription factors. It is essential for the development of the CNS particulary for the generation of granule cells in the hippocampus and cerebellum (Miyata et al., 1999). Enviromental signals regulate adult neurogenesis, at least in part through the activation of NeuroD1 (Deisseroth et al., 2004). Transcription activation of NeuroD1 is dependent on the Wnt/β-catenin activation. Gene promoter of NeuroD1 has an overlapping DNA-binding site for Sox2 and TCF/Lef, thus the activation of this gene also implies activation of the canonical Wnt pathway and removal of Sox2 repression from the NeuroD1 promoter. The activation of these genes by implication involves activation of the canonical Wnt signalling pathway (Kuwabara et al., 2009).

b) **Prospero homeobox protein 1**: is a protein, that is encoded by the *PROX1* gene in humans. This protein is produced primarily in the DG in the mouse, and in the DG and

white matter in humans. Prospero homeobox protein 1 has previously been shown to be important for lens development (Wigle et al., 1999), lymphangiogenesis (Wigle and Oliver, 1999), differentiation of ceratin spinal cord interneurons (Misra et al., 2008), and very recently, in hippocampal genesis of GCs (Lavado et al., 2010). It is also Wnt target gene that could be relevant for the neurogenic effect of the Wnt/β-catenin signalling pathway. It is expressed in newborn and mature GCs and it is required for the proper differentiation and survival of newborn GCs, but not for the maintenance of GCs after they have fully matured (Karalay et al., 2011).

c) **The promoter of long interspersed element-1** (L1): is abundant retrotransposon that comprises about 20% of mammalian genomes. Human genome is estimated to contain 80-100 retrotransposition-component L1s, and about 10% of these elements are classified as highly active. By comparison, the mouse genome is estimated to contain at least 3000 active L1s. Interestingly, the promotor region of L1s is actively retrontrasposed during neurogenesis, and it contains dual binding sites for Sox2 and TCF/LEF. Therefore, Wnt signalling pathway activation could upregulate the expression of genes adjacent to the L1 loci that may be relevant for neurogenesis such as DCX (Muotri et al., 2005).

1.5 Electrophysiological identification of cells

In 1972, S. J. Singer and G. L.Nichols introduced the fluid mosaic model of the plasma membrane according to which the biological membrane is considered as a two-dimensional liquid in which lipid and protein molecules diffuse more or less easily (Figure 9) (Singer and Nicolson, 1972). This led to conclusions that the membrane is selectively permeable and able to regulate the molecules to go inside or outside of the cell. Small molecules or ions, such as O_2, CO_2, and NO can move across the cell membrane by diffusion, which represents passive transport proceses. Conversely, nutrients, such as sugars or amino acids are not able to move across the plasma membrane by the diffusion, and are transported by the transmembrane protein channels and transporters. The type and number of ion channels determines how the cell reacts to signals from extracellular medium and what are active properties of the cell membrane.

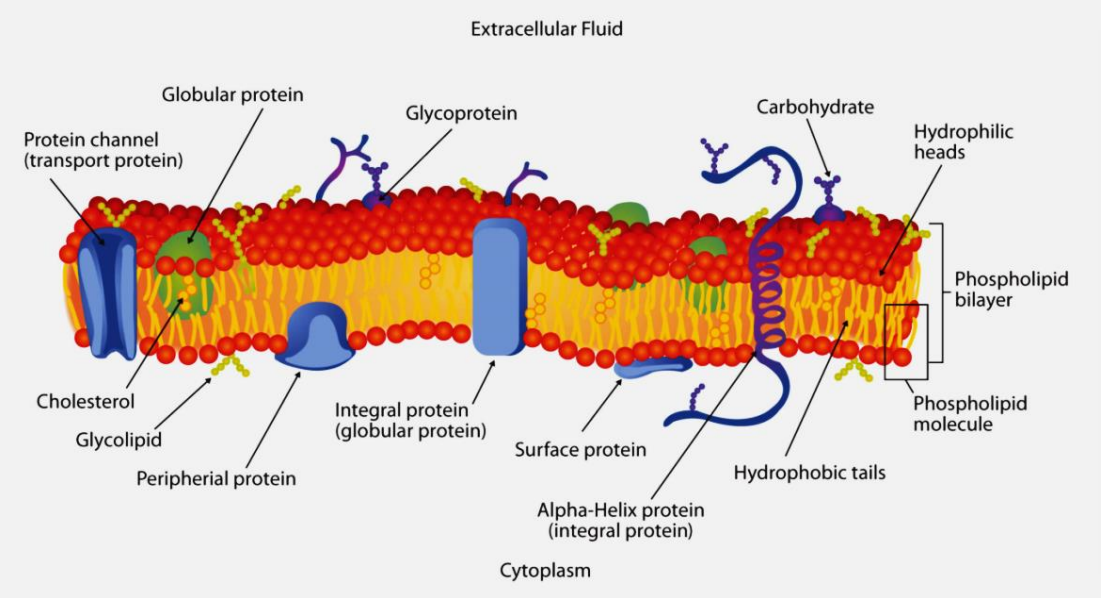

Figure 9: The structure of the cell membrane. The plasma membrane consists of phospholipid bilayer with embedded proteins. Proteins are interspersed among phospholipids. Two types of proteins can be found in the membrane: peripheral/extrinsic or integral/intrinsic. Peripheral proteins are attached loosely, while integral proteins partially permeate the bilayer or span the membrane entirely. These proteins are usually needed for transport across the cell membrane. Also glycoproteins are interspersed among phospholipids. They have carbohydrate chains bound to peripheral proteins and hydrophilic regions of intrinsic proteins. In the membrane, there are localized also glycolipids and cholesterol. Glycolipids have carbohydrates attached to fats. Cholesterol is interspersed among proteins and is a essential molecule in maintaining membrane fluidity[1].

[1]**Taken from:** *http://2012books.lardbucket.org/books/introduction-to-chemistry-general-organic-and-biological/s20-03-membranes-and-membrane-lipids.html*

1.5.1 Passive properties of the cell membrane

Passive membrane propertied include the membrane potential, capacitance of the membrane, and membrane input resistance.

Membrane potential (V_m) is defined as the difference in electric potential between the interior and the exterior of the cell. The membrane potential arises, because the plasma membrane is not permeable for all ions, primarily for ions as Na^+, $K^+$and Cl^-. Consequently, ion concentration in the interior and the exterior of the cell is not the same. The membrane potential has two main functions in the cell: provides energy for the cell to operate a variety of molecular mechanisms and it is used for transmitting signals between different parts of an electrically excitable cell, such as neurons or muscle cells. Signals are generated by opening or closing of ion channels at one point in the membrane and this operation produces a local change in the membrane potential. Subsequently, the change in the electric field is very quickly recognized by either adjacent or more distant ion channels in the cell membrane. These channels are opened or closed as a result of the potential change, which reproduces the signal. Typical membrane potential values range from -50 to -90mV, depending on the cell type. The unit of the membrane potential is milivolt (mV).

Membrane capacitance (C_m) acts as a capacitor. The capacitance arises because the lipid bilayer is so thin that accumulation of charged particles on one side gives rise to an electrical force that pulls oppositely charged particles towards the other side. The unit of the membrane capacitance is the farad (F), and cells have capacitance in orders of picofarads (pF). The value of capacitance is relative. It depends on molecules that are embedded in it, so it has a more or less invariant value, estimated at about 2 $\mu F/cm^2$. Membrane capacitance is mainly used for obtaining current density (current amplitude divided by membrane capacitance (pA/pF), but also for estimating changes in the size of the cell.

Membrane input resistance (IR) reflects the state of membrane channels. A low input resistance implies open channels, while high values of input resistance indicate closed channels. The unit of membrane input resistance is the ohm (Ω). Generally, the input resistance reaches high values in neurons (250-1500 MΩ), while in glial cells it is much lower, 30-100 MΩ.

1.5.2 Patch clamp

In the late 1970s Erwin Neher and Bert Sakmann came up with a patch clamp, a unique laboratory technique. This technique allows to study a single or multiple ion channels in cells. Patch clamp technique is primarily useful for studying of excitable cells: neurons, muscle fibers, pancreatic beta cells or cardiomyocytes, however, it is possible to use it for many types of cells to estimate their passive membrane properties and typical current profiles. This method uses a glass micropipette with the diameter of approximately 1 μm as a recording electrode. The microppipete is filled with a solution that imitates the intracellular fluid. Moreover, it can contain ligands or other substances which can interact with ion channels and thus influence their functioning in the cell membrane. The patch clamp technique has many variations:

a) **Cell-attached patch**: he borosilicate pipette is sealed onto the cell membrane and the so-called "gigaseal" is reached, while the cell membrane is still intact. This facilitates the recording of currents through single, or only a few, ion channel within the patch of the membrane captured by the pipette.

b) **Inside-out patch** : when a patch of membrane is attached to the patch pipette, and subsequently detached from the rest of the cell, this configuration is called inside-out. Here, the cytosolic surface of the membrane is exposed to the extracellular media. An advantage of this method is that have an acess to the intracellular side of the membrane, which can be easily influenced by drugs and chemicals. Using this method, channels, activated by intracellular ligands, can be studied employing a wide range of ligand concentrations.

c) **Whole-cell patch**: involves recording currents over the membrane of the entire cell. The pipette is left in place on the cell, like in cell-attached configuration, but more suction is applied to rupture the membrane at the contact with the pipette, an access from the interior of the pipette to the intracellular space of the cell. After the pipette is attached to the cell, there are two possibilities of breaking the membrane. One is to apply more suction as the amount and duration of the suction depends on the type of the cell an on the size of the pipette. The other method requires a large current pulse to be sent through the electrode (Figure10).

d) **Outside-out patch**: measurements employing the outside-out configuration begin as in the whole-cell configuration. However after the whole-cell configuration is formed, the electrode is carefully withdrawn from the cell, which allows a bleb of membrane. When the pipette is pulled away from the membrane, the bleb is detached from the cell and reformed as a convex membrane on the end of the pipette. The original outside of the membrane face outward from the pipette. This configuration gives the opportunity to asses the properties of ion channels since we can easily expose them to different solutions on the extracellular surface of the membrane.

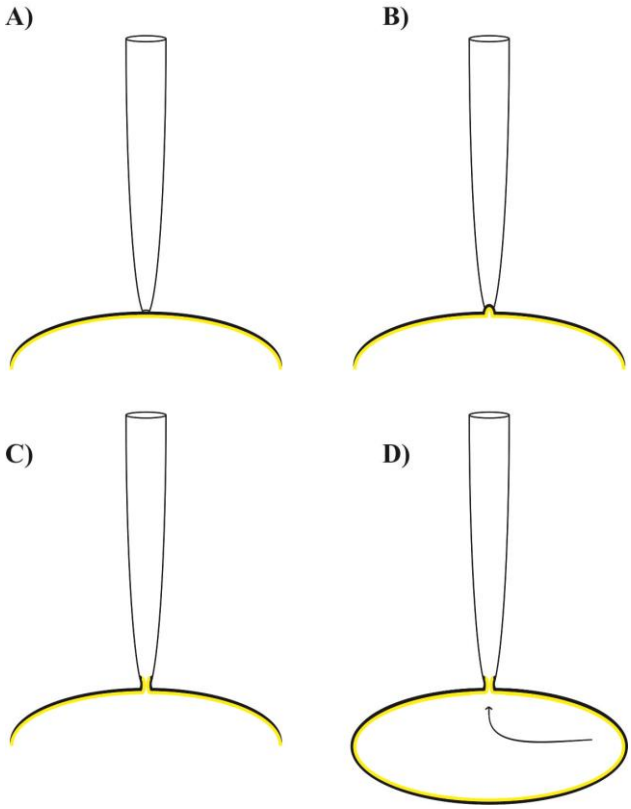

Figure 10: The patch clamp technique in the whole-cell type of configuration. **A)** The glass pipette is sealed onto the cell membrane. **B)** The so-called "gigaseal" is reached, but the cell membrane is still intact. **C)** More suction is applied and the membrane is ruptured. **D)** Electric currents passing through the membrane are being measured.

1.5.3 Membrane properties of neural cells

In situ, cells of the CNS: B-cells (NSCs),C-cells (transit amplifying cells), A-cells (neuroblasts), astrocytes, neurons, OPCs (NG2 glial cells) and oligodendrocytes, exhibit various properties of the cell membrane. Using the patch clamp technique, usually we distinguish four types of K^+ currents:

a) **K_A currents:** rapidly activating and inactivating outwardly rectifying K^+ currents. These currents are typical for neurons, transit amplyfying cells/C-cells and oligondendrocyte precursor cells/NG2 glial cells.
b) **K_{DR} currents:** delayed outwardly rectifying K^+ currents. These currents were found in NS/PCs/B-cells, transit amplifying cells/C-cells, neuroblasts/A-cells and neurons.
c) **K_{IR} currents:** inwardly rectifying K^+ currents. K_{IR} channels occur mainly in C-cells and astrocytes.
d) **Na^+ currents:** it is possible to find these currents in neurons or also in OPCs/NG2 glial cells.

B-cells (NSCs) give rise to C-cells. It is specific for these cells that they proliferate slowly and permanently. The plasma membrane of B-cells contains channels that display time and voltage-independent K^+ currents and delayed outwardly rectifying K^+ currents (K_{DR}) with small current density. These cells have high membrane potential (-70 to -90 mV) and low input resistance, circa 30 MΩ (Jelitai et al., 2007).

C-cells (transit amplifying cells) are produced from NS/PCs by asymmetric division. They are non-proliferating cells in the SVZ. The plasma membrane of C-cells expresses channels displaying K_{IR} and K_{DR} currents. Moreover they have also K_A currents. The membrane potential of C-cells is in the range from -70 to -80 mV. Their input resistance is around 250 MΩ (Jelitai et al., 2007).

A-cells (neuroblasts) are derived from C-cells in the SVZ and they migrate along the RMS to the OB. They express K_{DR} currents but they do not express K_{IR} currents. Many A-cells have Na^+ channels, but they are unable to generate action potentials (Wang et al., 2003). For these cells, low membrane potential, of approximately -50 mV, and high input resistance, around 4MΩ, are characteristic.

Membrane properties of *neurons* are very specific as these cells are specialized to the signal transmission. Neurons have many voltage-dependent Na^+ channels in their cell membrane. Na^+ channels play a key role in action potential generation. Repolarization of the plasma membrane is ensured by the presence of voltage-dependent K^+ channels, especially K_A and K_{DR} currents. When K^+ channels are activated and in the plasma membrane is an outward current of K^+ ions, returning the electrochemical gradient to the resting state. The cell membrane of neurons has the input resistance of around 300-600 MΩ and the membrane potential of approximately -60mV (Bean, 2007).

High troughut of K^+ ions across the membrane is typical for *astrocytes*. One of the main functions of astrocytes is to maintain the concentration of K^+ around neurons and therefore, their membrane is highly permeable for K^+ ions.. Astrocytes express K_{IR} currents and after depolarization and hyperpolarization, they show passive conductivity for K^+. In the immature nervous system, precursors of astrocytes are also often found. These cells have voltage-dependent K^+ channels and voltage-dependent Na^+ channels (Chvátal et al., 1999). The input resistance of the membrane in astrocytes is from -30 to -100 MΩ and the membrane potencial approximately from -70 to -80mV (Ransom and Sontheimer, 1992).

Oligodendrocyte precursor cells also known as NG2 glial cells are a subtype of glial cells in the CNS. These cells can be precursors for oligodendrocytes, but also can differentiate into neurons or astrocytes. Depolarization activates voltage-dependent K_A and K_{DR} currents in OPCs. Conversely, hyperpolarization activates K_{IR} currents in these cells. In some cases, Na^+ channels were also found in OPCs (Lin and Bergles, 2002). The average input resistance of OPCs is from 200 to 500 MΩ and the membrane potential is -70mV.

Oligodendrocytes provide support and insulation to axons in the CNS. The plasma membrane of oligodendrocytes is also highly permeable for K^+ ions. The membrane input resistance of oligodendrocytes is 200-350 MΩ and the value of membrane potential is -60mV. Oligodendrocyte precursors have voltage-dependent K^+ channels like astrocytes, but they do not display voltage-dependent Na^+ channels (Chvátal et al., 1999).

1.6 Immunocyto/histochemical identification of neuronal cells

An immunocyto/histochemical method are often used for identification of neuronal cells. It is a powerful method for localizing specific antigens in formalin-fixed, paraffin-embedded tissues (Taylor and Burns, 1974). Using antibodies against various cell components, investigators are able to identify cells displaying a neuronal phenotype and, moreover, collect information regarding their morphological characteristics and expression of specific proteins :

a) **Glial fibrillary acidic protein**: is a protein type III intermediate filament, which is used as a marker of astrocytes (Jacque et al., 1978) and ependymal cells (Roessmann et al., 1980). Besides CNS, it is also expressed in human keratinocytes (von Koskull, 1984), osteocytes and chondrocytes (Kasantikul and Shuangshoti, 1989), satelite cells of pancreas (Apte et al., 1998) or Muller cells of retina (Goel and Dhingra, 2012). Expression of GFAP mRNA is rapidly induced following acute brain injury and modified by neurological disease (Eng et al., 2000). In addittion, transcription of GFAP mRNA increases with age (Nichols et al., 1993).

b) **Vimentin:** is a marker of NSCs (Seri et al., 2004) and certain subpopulation of reactive astrocytes (Anderova et al., 2011). It is a protein of typ III intermediate filament, charakteristic for leucocytes, blood vessels endothelial cells, some epithelial cells and mesenchymal cells. This protein plays a significant role in supporting and anchoring the position of the organelles in the cytosol. It is attached in the nucleus, mitochondria and endoplasmatic reticulum (Katsumoto et al., 1990).

c) **Nestin:** is type VI intermediate filament protein (Guérette et al., 2007). This protein is expressed by many cell types in developing CNS, beacause it mainly labels newly derived cells. In adult organisms, it is expressed, for example, in the neuron precursor cells of the SGZ, but also in reactive astrocytes and proliferating NG2glia (Anderova et al., 2011).

d) **Doublecortin**: is a microtubule binding protein. Analysis of newly generated cells showed that DCX is transiently expressed in C-cells (transit amplifying cells) and newly generated A-cells (neuroblasts). This protein serves as a marker for adult neurogenesis. Neural stem/progenitor cells begin to express DCX while actively dividing, and their neuronal daughter cells continue to express DCX for 2-3 weeks as

the cells mature into neurons. Downregulation of this protein begins after 2 weeks, and concides with the onset of NeuN expression, which represents neuronal maturation (Brown et al., 2003).

e) **Microtubule associated protein 2**: stabilizes microtubules growth by crosslinking microtubules with intermediate filaments and other microtubules. Multiple forms of MAP2 are expressed during development. For example in rodents, MAP2-b and MAP2-c are expressed during fetal CNS development during which MAP2c functions to maintain the cytoskeleton in a more flexible state (Shafit-Zagardo and Kalcheva, 1998).

f) **Neural glial antigen 2** (chondroitin sulphate proteoglycan 4): proteoglycans are a familly of moleculs, that contain gylcosaminoglycan chains covalently linked to their core proteins. They are found in the extracellular matrix or on the cell surface and have multiple functions: cell integration and migration (Rapraeger et al., 1986), cell adhesion (Yamagata et al., 1989), and cell proliferation (Yamaguchi and Ruoslahti, 1988). Neural glial antigen 2 (NG2) is cell surface proteoglycan, primarily found to be expressed by neural cells (Stallcup and Beasley, 1987). NG2 is a marker of proliferating progenitor cells (Nishiyama et al., 1991).

g) **Calcium binding protein β**: the localization of calcium binding protein β (S100β) is in the cytoplasm, and in the nucleus. This protein regulates many cellular processes such as progression of cell cycle or differentiation. It is expressed by NSCs, astrocytes, NG2 glial cells or Schwann cells (Cocchia et al., 1981).

1.7 Western blot

Western blot also called protein immunoblot is a analytical technique used to identify specific proteins in a sample of tissue extract. These technique comprises gel electrophoresis to isolating proteins by the length of the polypeptide. The proteins can be isolated based on their molecular weight, isoelectric point, electric charge or also a combination of all three factors. Most widely used kind of electrophoresis gels are polyacrylamide gels and buffers loaded with sodium dodecyl sulfate. Subsequently proteins are transferred to the nitrocellulose or polyvinylidene fluoride membrane, which is used for protein identification with the antibodies specific to the target protein (Figure 11).

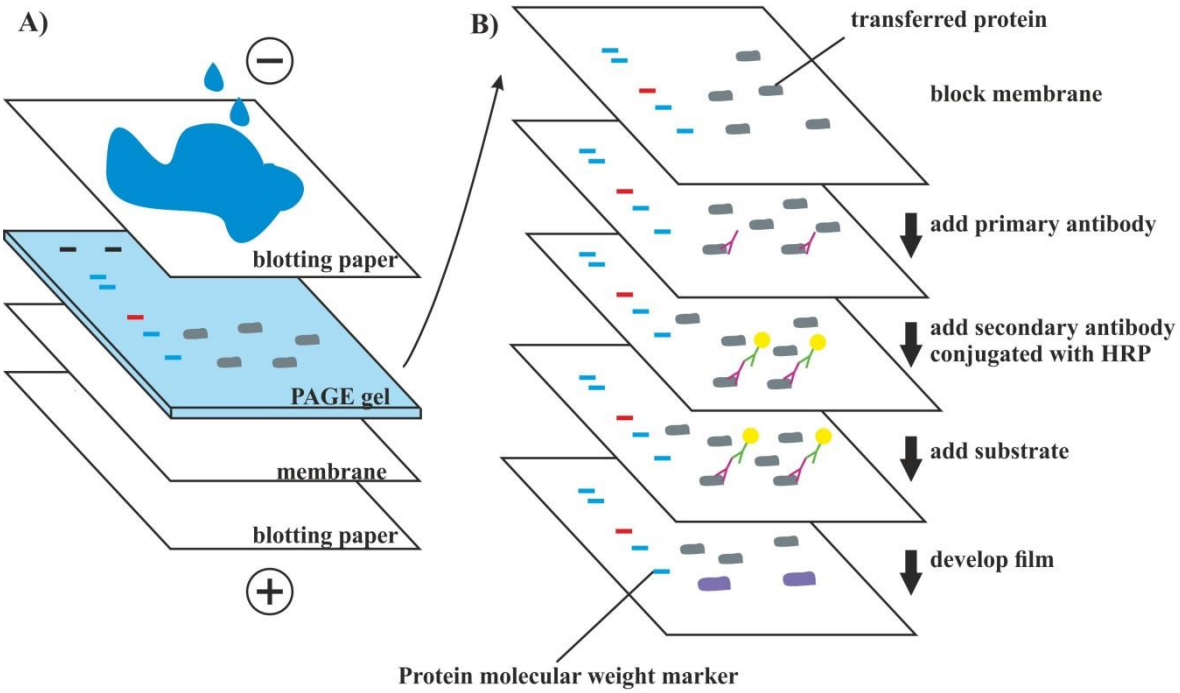

Figure 11: **Western blot workflow**. **A)** A PAGE gel-membrane sandwich between two sheets of filter paper. **B)** Western blot comprises steps as follows: Blocking membrane to prevent non-specific binding of primary antibodies. Incubating the membrane with primary antibodies. Incubating the membrane with secondary antibodies conjugated with horseradish peroxidase. Incubating the membrane with substrate which reacts with the enzyme and reveals where the protein of interest is localized. **Abbreviations**: **HRP**= horseradish peroxidase, **PAGE**= polyacrylamide gel electrophoresis.

2 MATERIAL AND METHODS

2.1 Transgenic animals

Neonatal (P0-2) and adult mice (P50-56) were used in this study. Rosa26-tdTomato-EGFP/dnTCF4(Janeckova et al., 2016) and Rosa26-Dkk1 (Wu et al., 2008) mice as well as a mouse with targeted allele Catnb-lox^{Ex3} (Harada et al., 1999) were crossbred with a universal Cre deletor mouse Rosa26-creERT2 (Ventura et al., 2007), which enabled either the inhibition of Wnt signalling at the nuclear (Rosa26$^{dnTCF4/creERT2}$; further termed dnTCF4) or membrane level (Rosa26$^{Dkk1/creERT2}$; further termed Dkk1) or its activation in the cytoplasm (Catnb$^{del(Ex3)/+}$Rosa26$^{+/creERT2}$; further termed Ex3) (Figure 12). The Wnt signalling manipulation was facilitated by the addition of 4-hydroxytamoxifen (4OHT; 1 μM; Sigma-Aldrich, St. Louis, MO, USA) dissolved in ethanol into the differentiation medium. Cells that had not been treated with 4OHT were used as the controls.

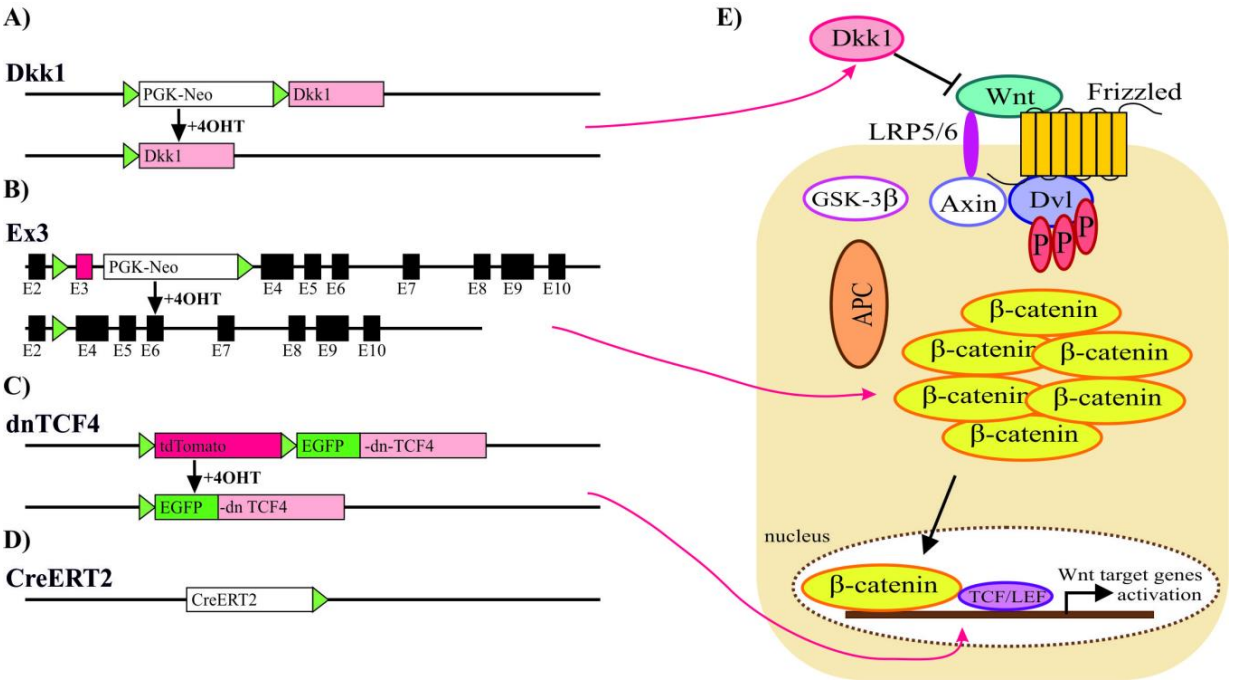

Figure 12: Transgenic mouse strains and the canonical Wnt/β-catenin signalling pathway. dnTCF4 and Dkk1 mice as well as Ex3 mice were crossbred with a Cre deletor mouse CreERT2, which enabled the inhibition of Wnt signalling at the nuclear/membrane level and its activation in the cytoplasm, respectively (pink arrows). **A)** Suppression of Wnt signalling at the membrane level due to the over-expression of a secreted Wnt inhibitor, Dkk1. **B)** Activation of the pathway caused by the production of a stable form of β-catenin. The Cre-mediated excision of the exon 3 (E3, red rectangle) removes the amino acid sequence

responsible for the degradation of the protein and thus β-catenin aberrantly activates the Wnt target genes. **C)** The Wnt-responsive transcription in the nucleus blocked by a dominant negative form of the T-cell factor protein. **D)** Cre deletor mouse Rosa26-CreERT2 carries the gene encoding tamoxifen-inducible Cre recombinase fused with a modified form of the estrogen receptor. **E)** The Wnt/β-catenin signalling pathway and its key components. **Abbreviations: Cre**= Cre recombinase; **pA**= polyadenylation site; **PGK-Neo**= neomycin resistance cassette; **E2 – E10**= exon 2 – 10; **EGFP**= enhanced green fluorescent protein; dn-**TCF4**= dominant negative T-Cell Factor; **CreERT2**= Cre recombinase/modified form of the estrogen receptor; **Wnt**= Wingless/Integrated; **Dkk1**= Dickkopf 1; **LRP5/6**= Low-density Lipoprotein 5/6; **Dvl**= Dishevelled; **P**= phosphorylated site; **APC**= Adenomatous Polyposis Coli; **GSK-3β**= Glycogen Synthase Kinase 3β; **TCF/LEF**= T-Cell Factor/Lymphoid Enhancer Factor.

2.2 Cell culture

Primary cultures were prepared from NS/PCs isolated from neonatal (frontal lobe) and adult mouse brains (SVZ of lateral ventricles). Adult mice were deeply anesthetized with sodium pentobarbital (PTB, 100mg/kg, i.p.) and perfused transcardially with cold (4–8 °C) isolation solution containing (in mM): 110 NMDG-Cl, 2.5 KCl ,24.5 $NaHCO_3$, 1.25 Na_2HPO_4, 0.5 $CaCl_2$, 7 $MgCl_2$ and 20 glucose. (osmolality 290 ± 3 mOsmol/kg). The brain was isolated and sliced in ~0.5 mm coronal sections using a vibrating microtome HM650V (MICROM International GmbH, Walldorf, Germany), and the SVZ was dissected from the lateral walls of the ventricular zone. The tissue was incubated with continuous shaking at 37 °C for 45 min in 1 ml of papain (20U/ml) and 50 µl DNAase (both from Worthington, Lakewood, NJ). After papain treatment, 1 ml of trypsin inhibitor (Sigma-Aldrich, St. Louis, MO, USA) was added to inactivate papain activity. Single cell suspension was centrifuged at 1020 for 3 minutes and 1 ml of proliferation medium containing Neurobasal-A medium (Life Technologies, Waltham, MA, USA) supplemented with B27 (2%; Life Technologies, Waltham, MA, USA), Glutamine (2 mM; Sigma-Aldrich, St. Louis, MO, USA), Primocin (100 µg/ml; Invitrogen, Toulouse, France) and growth factors bFGF (10 ng/ml) and EGF (15 ng/ml; both PeproTech, Rocky Hill, NJ, USA) was added. The cells were mechanically dissociated by gentle trituration using a 1 ml pipette. The cell suspension was subsequently transferred through a 70 µm cells strainer into a 100 mm Petri dish containing 9 ml of proliferation medium.

In neonatal mice, after decapitation the brains were quickly dissected out and the frontal lobe of the brain was isolated and transferred into proliferation medium containing Neurobasal-A medium (Life Technologies, Waltham, MA, USA) supplemented with B27 (2%; Life Technologies, Waltham, MA, USA), Glutamine (2 mM; Sigma-Aldrich, St.

Louis, MO, USA), Primocin (100 µg/ml; Invivogen, Toulouse, France) and growth factors bFGF (10 ng/ml) and EGF (10 ng/ml; both PeproTech, Rocky Hill, NJ, USA). Using a 1 ml pipette, the tissue was mechanically dissociated and the cell suspension subsequently transferred through a 70 µm cells strainer into a 100 mm Petri dish containing 9 ml of proliferation medium.

The adult and neonatal cells were cultured as neurospheres at 37 °C and 5% CO_2. After 7-14 days of *in vitro* proliferation, the neurospheres were collected and transferred into a 12 ml Falcon tube and centrifuged at 1020 RCF for 3 minutes. The supernatant was discarded and 1 ml of trypsin (Sigma-Aldrich, St. Louis, MO, USA) was added. After 3 minutes, 1 ml of trypsin inhibitor (Sigma-Aldrich, St. Louis, MO, USA) was added to the dissociated cells to block the trypsinization. Consequently, 100 µl of the cell suspension was used to count cells in the hemocytometer. The rest of the cell suspension was centrifuged at 1020 RCF for 3 minutes. The cells were plated on coverslips coated with poly-L-lysine (Sigma-Aldrich, St. Louis, MO, USA) at the cell density $6x10^4$ cells/cm^2 and treated with differentiation medium (the same composition as the proliferation medium, but without EGF, and with 20 ng/ml bFGF). To estimate the impact of Wnt signalling inhibition/activation during differentiation, cells were cultured either in differentiation medium without (controls – intact Wnt pathway) or with (Z)-4-hydroxytamoxifen in ethanol (4OHT; 1uM; Sigma-Aldrich, St. Louis, MO, USA). The cells were maintained at 37 °C and 5% CO_2, with medium exchange on every third day. After 8-9 days of *in vitro* differentiation, the cells were used for electrophysiological measurements, immunocytochemistry Western blot analysis, where ethanol-treated (controls) and 4OHT-treated cultures were compared.

2.3 Patch-clamp recording

Cell membrane currents were recorded 8-9 days after the onset of differentiation using the patch-clamp technique in the whole-cell configuration. Recording pipettes with a tip resistance of 8–12 MΩ were made from borosilicate capillaries (Sutter Instruments, Novato, CA, USA) using a P-97 Brown-Flaming micropipette puller (Sutter Instruments, Novato, CA, USA). Recording pipettes were filled with intracellular solution containing (in mM): 130 KCl, 0.5 $CaCl_2$, 2 $MgCl_2$, 5 EGTA, 10 HEPES (pH 7.2). To visualize the recorded cells, the intracellular solution contained Alexa Fluor hydrazide 488 (A488; Molecular Probes, Carlsbad, CA, USA) (Figure 13).

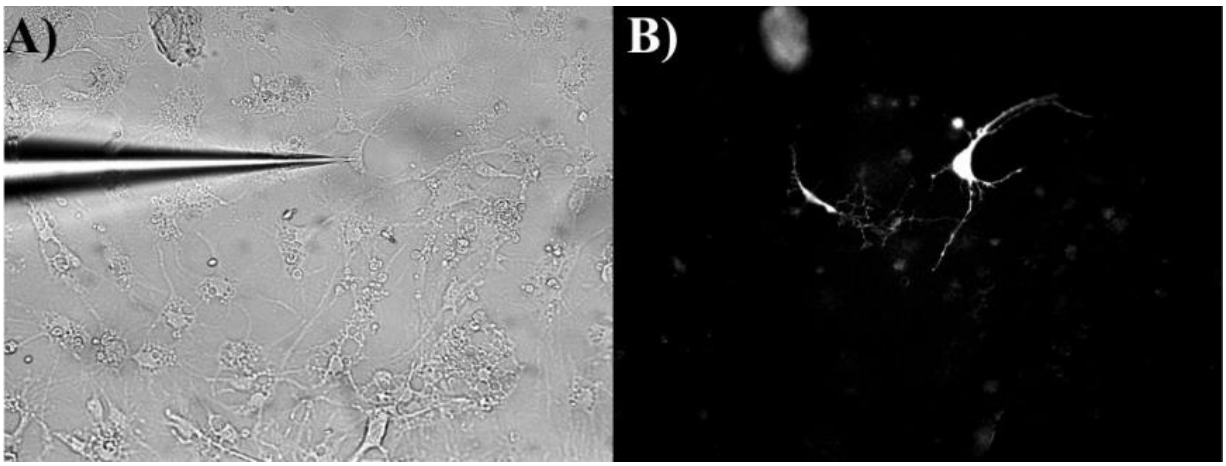

Figure 13: Patch clamp technique in the whole-cells configuration. A) Glass micropipette filled with fluorescent dye (alexa 488) attached to a cell. **B)** Fluorescently labelled cell after measurement.

The labelled cells were used for further post-recording immunocytochemical identification. All recordings were made in artificial cerebrospinal fluid (aCSF) containing (in mM): 122 NaCl, 3 KCl, 1.5 $CaCl_2$, 1.3 $MgCl_2$, 1.25 Na_2HPO_4, 28 $NaHCO_3$, 10 D-glucose (osmolality 300 ± 5 mmol/kg). The solution was continuously gassed with a mixture of 95% O_2 and 5% CO_2 to maintain final pH of 7.4. All recordings were made on coverslips perfused with aCSF at room temperature. Electrophysiological data were measured with 10 kHz sample frequency using an EPC9 or EPC10 amplifier controlled by PatchMaster software (HEKA Elektronik, Lambrecht/Pfalz, Germany) and filtered using a Bessel filter. The coverslips with cells were transferred to the recording chamber of an upright Axioscop microscope (Zeiss, Gottingen, Germany) equipped with electronic micromanipulators (Luigs & Neumann, Ratingen, Germany) and a high-resolution AxioCam HR digital camera (Zeiss, Gottingen, Germany).

The resting V_m was measured by switching the EPC9 or EPC10 amplifier to the current-clamp mode. Using FitMaster software (HEKA Elektronik, Lambrecht/Pfalz, Germany), the membrane resistance (IR) was calculated from the current value 40 ms after the onset of the depolarizing 10 mV pulse from the holding potential of -70 mV to -60 mV for 50 ms. C_m was determined automatically from the Lock-in protocol by PatchMaster. Current patterns were obtained by hyper- and depolarizing the cell membrane from the holding potential of -70 mV to the values ranging from -160 mV to 40 mV at 10 mV intervals. Pulse duration was 50 ms. In order to isolate the K_{DR} current components, a voltage step from -70 to -60 mV was used to subtract the time- and voltage-independent currents as

described previously (Anderová et al., 2006). To activate the K_{DR} currents only, the cells were held at -50 mV, and the amplitude of the K_{DR} currents was measured at 40 mV at the end of the pulse. K_{IR} currents were determined at -160 mV at the end of the pulse. The fast activating and inactivating K_A currents were isolated by subtracting the current traces clamped at -110 mV from those clamped at -50 mV, and its amplitude was measured at the peak value. Current densities were calculated by dividing the maximum current amplitudes by the corresponding C_m values for each individual cell. Tetrodotoxin (TTX)-sensitive Na^+ currents were isolated by subtracting the current traces measured in a solution containing 1 μM tetrodotoxin (TTX; Alomone Labs, Jerusalem, Israel) from those measured in the absence of TTX. Na^+ current amplitudes were measured at the peak value. Action potentials were obtained in the current-clamp mode. Current values ranged from 50 pA to 1 nA at 50 pA intervals. Pulse duration was 300 ms.

After recording, the coverslips were fixed in phosphate buffer (PB; 0.2 M; pH 7.4) containing 4% paraformaldehyde for 9 minutes and then transferred to phosphate-buffered saline (PBS) (10 mM; pH 7.2) for post-recording identification using immunocytochemistry.

2.4 Immunocytochemistry

Primary cultures attached to PLL-coated coverslips were fixed in 4% paraformaldehyde solution in 0.2 M PB buffer (pH 7.4) for 9 minutes and kept in 10 mM PBS at 4°C for further processing. Coverslips were incubated in a blocking solution containing 5% Chemiblocker (Millipore, Billerica, MA, USA) and 0.5% Triton X-100 (Sigma-Aldrich, St. Louis, MO, USA) in 10 mM PBS at 4°C for 2 hours. Next, they were incubated overnight at 4°C with primary antibodies in PBS containing 0.2% Triton X-100. After the overnight incubation, three 10-minute washes with PBS were performed, followed by incubation with secondary antibodies for two hours at 4°C. For double labeling, a mouse monoclonal antibody directed against GFAP conjugated with Cy3 (1:800; Sigma-Aldrich, St. Louis, MO, USA) was subsequently applied and incubated overnight at 4°C. Afterwards, the coverslips were washed in PBS three times for 10 minutes. To visualize cell nuclei, the coverslips were incubated with 300 nM 4′,6-diamidino-2-phenylindole (DAPI) in PBS for 5 minutes at room temperature. Finally, the coverslips were mounted using Aqua Poly/Mount (Polysciences Inc., Eppelheim, Germany). An LSM 5 DUO spectral confocal

microscope (Zeiss, Gottingen, Germany) equipped with an Arg/HeNe laser was used for immunochemical analyses.

Table 1: Primary and secondary antibodies used for immunocytochemistry and Western blot analysis. **Abbreviations: ICC**= immunocytochemistry; **WB**= Western blot; **GFAP-Cy3**= glial fibrillary acidic protein coupled with the Cy3 fluorescent dye; **PDGFαR**= platelet-derived growth factor alpha receptor; **DCX**= doublecortin; **MAP2**= microtubule associated protein 2; **Non-pβ-catenin**= non-phosphorylated β-catenin; **β III tubulin**= β-tubulin isotype III; **GAM/GAR 488/594/660**= goat anti-mouse/rabbit IgG conjugated with Alexa Fluor 488/594/660.

.

Method	Primary antibody	Dilution	Manufacturer	Secondary antibody	Dilution	Manufacturer
ICC	GFAP-Cy3	1:800	Sigma-Aldrich, St. Louis, MO, USA	--	--	--
	PDGFαR	1:200	Santa Cruz Biotechnology, Dallas,	GAM/GAR 488/594/660	1:200	Molecular Probes, Carlsbad, CA, USA
	DCX	1:500	Santa Cruz Biotechnology, Dallas,			
	MAP2	1:800	Chemicon, Billerica, MA, USA			
WB	β-actin	1:1000	Santa Cruz Biotechnology, Dallas,	Horseradish peroxidase-conjugated secondary antibodies	1:5000	Jackson ImmunoResearch Laboratories, West Grove, PA, USA
	β-catenin	1:2000	BD Biosciences, San Jose, CA, USA			
	Non-pβ-catenin	1:300	Cell Signalling Technology, Danvers,			
	β III tubulin	1:400	Sigma-Aldrich, St. Louis, MO, USA			

2.5 Immunocytochemistry and quantification of β-catenin signal intensity

Immunocytochemical staining was performed as described previously (Doubravska et al., 2011) using mouse monoclonal antibody against β-catenin (BD Transduction Laboratories, San Jose, CA, USA), goat-anti-mouse secondary antibody conjugated with Alexa 488 dye and DAPI (Sigma-Aldrich, St. Louis, MO, USA). Twelve fluorescent microscopy images were taken from every cell type treated with ethanol only or 4-hydroxytamoxifen in ethanol. The Alexa 488 and DAPI fluorescent signal were analyzed using the ImageJ software (NIH, Bethesda, MD, USA) and the intensity of β-catenin staining was normalized to cell number in every slide. Obtained data were evaluated by Student's t-test.

2.6 Western blot

Cells were lysed in standard 1x RIPA buffer containing 25 mM Tris-HCl, pH 8.; 150 mM NaCl; 1% NP-40; 1% sodium deoxycholate; 0.1% SDS; 1 mM EDTA and supplemented

with inhibitors of proteases (Roche, Basel, Switzerland) and phosphatases (20 mM NaF; 1mM Na_3VO_4). Total protein content in the homogenates was determined using the Pierce BCA™ protein assay kit (Thermo Fisher Scientific, Waltham, MA, USA). Equal amounts of proteins supplemented with 100 mM dithiothreitol were subjected to SDS PAGE (10 – 15%), proteins were transferred onto nitrocellulose membrane (Hybond ECL 0.45 μM; Amersham, Little Chalfont, UK) and detected by specific antibodies combined with horseradish peroxidase-conjugated secondary antibodies (Jackson Immunoresearch, West Grove, PA, USA). Peroxidase activity was detected by ECL (Amersham, Little Chalfont, UK).

2.7 Data Analysis and Statistics

Data are presented as means ± S.E.M. (standard error of the mean) for n cells, unless otherwise stated. Student's unpaired t-test was used to determine significant differences between the experimental groups. Values of *$p < 0.05$ were considered significant, **$p < 0.01$ very significant and *** $p < 0.001$ extremely significant.

3 AIMS OF THE STUDY

The aim of this study was to elucidate the role of the canonical Wnt/β-catenin pathway in gliogenesis and neurogenesis *in vitro* in neonatal and adult NS/PCs. The study was focused on differentiation of NS/PCs employing three transgenic mouse strains enabling tamoxifen-inducible Cre-recombinase-mediated DNA recombination, which facilitates manipulation (inhibition/activation) of the Wnt signalling pathway *in vitro*. The phenotype of differentiated cells was analysed using the patch-clamp technique, immunocytochemical staining, and Western blot.

Specific aims of the project:

1. To verify the impact of DNA recombination on β-catenin levels and the Wnt target genes in neonatal and adult NS/PCs.
2. To assess the effect of Wnt signalling manipulation on NS/PCs differentiation isolated from neonatal and adult transgenic mice.
3. To elucidate the influence of Wnt signalling inhibition/activation on electrophysiological properties of differentiated NS/PCs isolated from neonatal and adult mice.

4 RESULTS

4.1 Neonatal neural stem/progenitor cells

4.1.1 Beta-catenin levels in differentiated neonatal neural stem/progenitor cells

To confirm that our *in vitro* approach using NS/PCs isolated from dnTCF4, Dkk1, and Ex3 transgenic mice represents a suitable tool for affecting the Wnt signalling pathway, we carried out immunocytochemical (Figure 14 and 15) and Western blot (Figure 16) analyses of differentiated neonatal NS/PCs for β-catenin, one of the main components of this pathway. After inhibiting the pathway in the nucleus (dnTCF4; Figure 14A and 15), there were no differences in the expression levels of the protein, however, Wnt signalling pathway suppression at the cell membrane (Dkk1; Figure 14B and 15) resulted in a marked decrease in the β-catenin expression. Moreover, activation of the Wnt signalling pathway (Ex3; Figure 14C and 15) confirmed the abundance of the β-catenin protein in the cytoplasm.

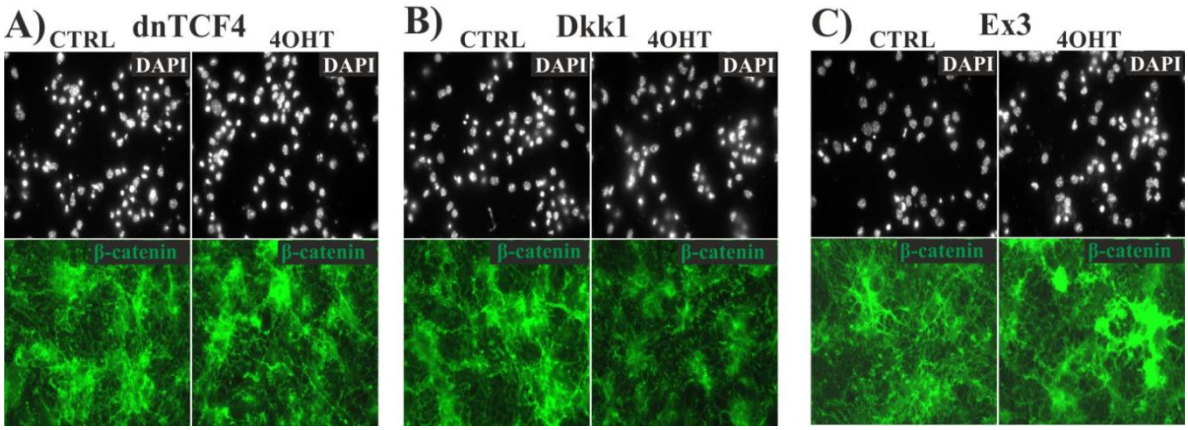

Figure 14: Beta-catenin staining in differentiated neonatal neural stem cells: A) Fluorescent images of β-catenin staining in differentiated NS/PCs derived from neonatal dnTCF4 mice with inhibited Wnt signalling pathway at the nuclear level in CTRL and 4OHT cultures. **B)** Fluorescent images of β-catenin staining in differentiated NS/PCs derived from neonatal Dkk1 mice with inhibited Wnt signalling pathway at the membrane level in CTRL and 4OHT cultures. **C)** Fluorescent images of β-catenin staining in differentiated NS/PCs derived from Ex3 mice with activated Wnt signalling pathway in the cytoplasm in CTRL and 4OHT cultures. **Abbreviations**: **4OHT**= tamoxifen-treated cultures; **CTRL**= control cultures; **DAPI**= 4',6-diamidino-2-phenylindole; **Dkk1**= NS/PCs derived from neonatal Dkk1 mice; **dnTCF4**= NS/PCs derived from neonatal dnTCF4 mice; **Ex3**= NS/PCs derived from neonatal Ex3 mice; **NS/PCs**= neural stem/progenitor cells; **Wnt**= Wingless/Integrated.

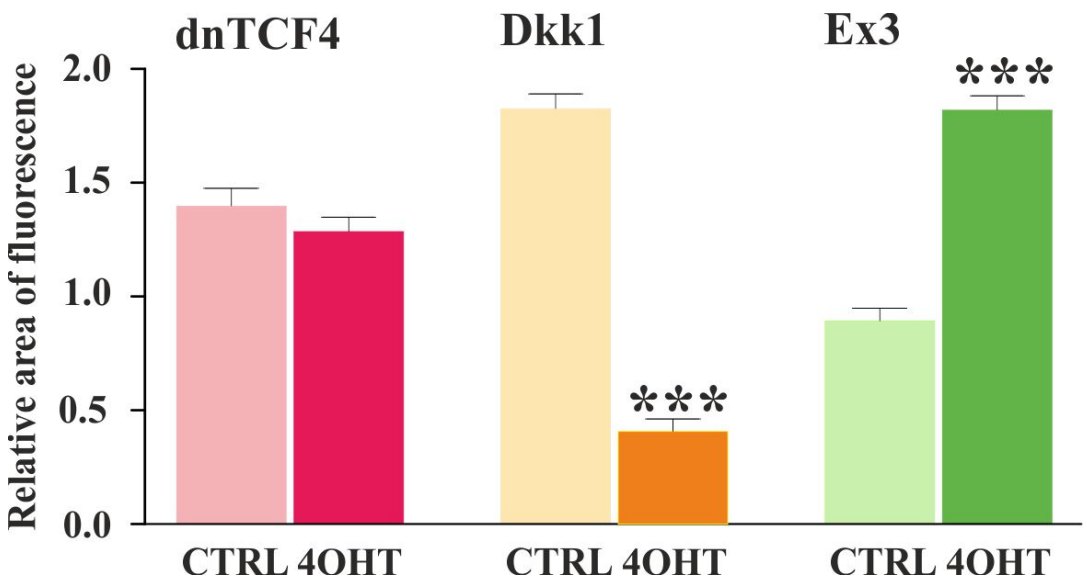

Figure 15: Quantification of β-catenin expression showing the proportion of area of positively-stained cells to DAPI-positive area (n=12). The values are represented as mean ± S.D. Statistical significance was calculated using t-test. ***,$p < 0.001$. Note a marked changes in β-catenin levels after Wnt inhibition or activation in differentiated NS/PCs from Dkk1 and Ex3 mice. **Abbreviations**: **4OHT**= tamoxifen-treated cultures; **CTRL**= control cultures; **Dkk1**= NS/PCs derived from neonatal Dkk1 mice; **dnTCF4**= NS/PCs derived from neonatal dnTCF4 mice; **Ex3**= NS/PCs derived from neonatal Ex3 mice.

Western blot analysis showed minor changes in β-catenin expression in the cells with inhibited Wnt signalling (Figure 16A and B). On the other hand, higher quantity of total protein and lower quantity of phosphorylated protein (Figure 16C) proved higher levels of a stable form of β-catenin in the cells. Using the ImageJ software (NIH, Bethesda, MD, USA), we estimated β-catenin-to-phosphorylated-β-catenin ratio for both treatments in all three mouse strains. After Wnt signalling pathway inhibition, the ratio decreased in differentiated neonatal NS/PCs derived from dnTCF4 and Dkk1 mice from 1.27 and 1.00 in controls to 0.84 and 0.85, respectively, while in differentiated neonatal NS/PCs derived from Ex3 mice, the ratio increased from 0.90 in control to 7.46 after Wnt signalling activation. Moreover, Western blot analysis revealed higher β III tubulin expression in the cells with activated pathway when compared to the controls.

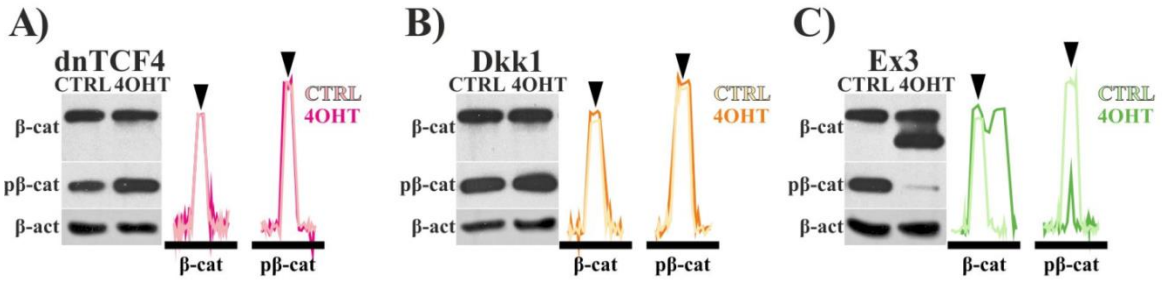

Figure 16: Western blot analysis of total and phosphorylated β-catenin (left) and intensity profiles representing the number and the size of the respective bands (right). Arrowheads mark the molecular weight of 92 kDa. **Abbreviations: 4OHT**= tamoxifen-treated cultures; **CTRL**= control cultures; **Dkk1**= NS/PCs derived from neonatal Dkk1 mice; **dnTCF4**= NS/PCs derived from neonatal dnTCF4 mice; **Ex3**= NS/PCs derived from neonatal Ex3 mice; **β-CAT**= β-catenin; **pβ-CAT**= phosphorylated β-catenin; **NS/PCs**= neural stem/progenitor cells**.**

4.1.2 Membrane properties of differentiated neonatal neural stem/progenitor cells

In order to estimate the impact of Wnt signalling pathway inhibition/activation on neonatal NS/PCs differentiation, we employed the patch-clamp technique in the whole-cell configuration to assess the current profiles of *in vitro* differentiated cells. Control (n=347) and 4OHT-treated (n=380) cells were subsequently divided into three groups according to their electrophysiological properties:

a) Flat-shaped cells (n=242) displayed passive time- and voltage-independent K^+ currents (passive current pattern; Figure 17A), and their average V_m was -86.38 ± 0.26 mV and IR was 81.62 ± 1.91 MΩ.

b) Round cells (n=289), expressing fast activating and inactivating K_A and K_{DR} (Figure 17C), were characterized by V_m of -72.04 ± 0.90 mV and high values of IR (1649.79 ± 44.05 MΩ).

c) Branched cells (n=196), with a complex current pattern, expressed K_{IR} currents, in addition to K_{DR} and K_A currents (Figure 17B) and their V_m was -85.78 ± 0.45 mV and IR was 218.56 ± 8.24 MΩ.

Post-recording immunocytochemical identification revealed that the majority of the cells expressing passive current pattern were GFAP-positive, while most of the cells displaying outwardly rectifying currents were DCX/MAP2-positive. Complex currents were expressed mainly by PDGFαR-positive cells (Figure 18 A, B, C, D).

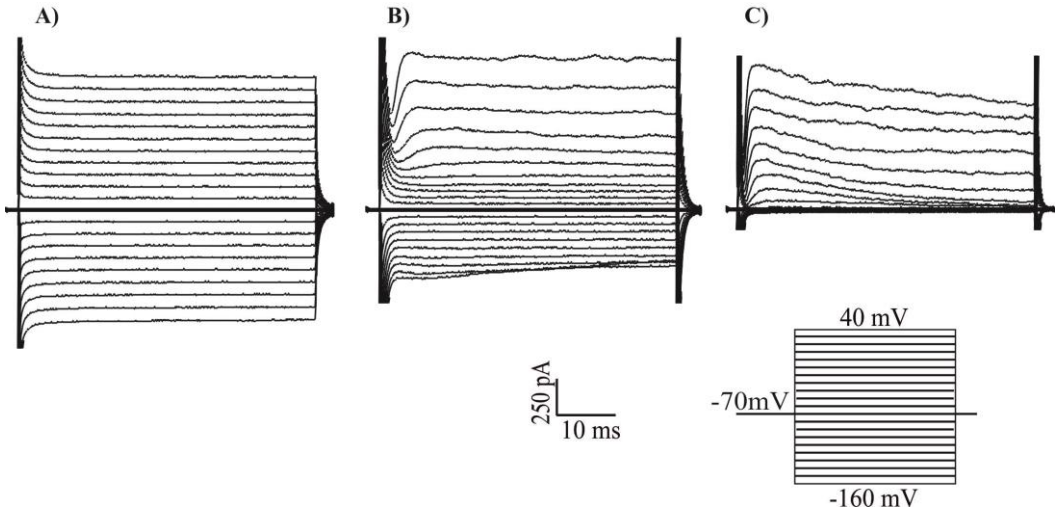

Figure 17: Typical current profiles of differentiated neural stem cells. A) Cells with a passive current pattern display predominantly time- and voltage-independent K^+ currents and small amplitudes of delayed K_{DR} and K_{IR}. **B)** Cells displaying a complex current profile express fast activating and inactivating K_A together with K_{DR} and K_{IR} currents. **C)** Cells with an outwardly rectifying current pattern express only K_A and K_{DR} currents. **Abbreviations: K_A**= fast activating and inactivating outwardly rectifying K^+ currents; **K_{DR}**= outwardly rectifying K^+ currents; **K_{IR}**= inwardly rectifying K^+ currents.

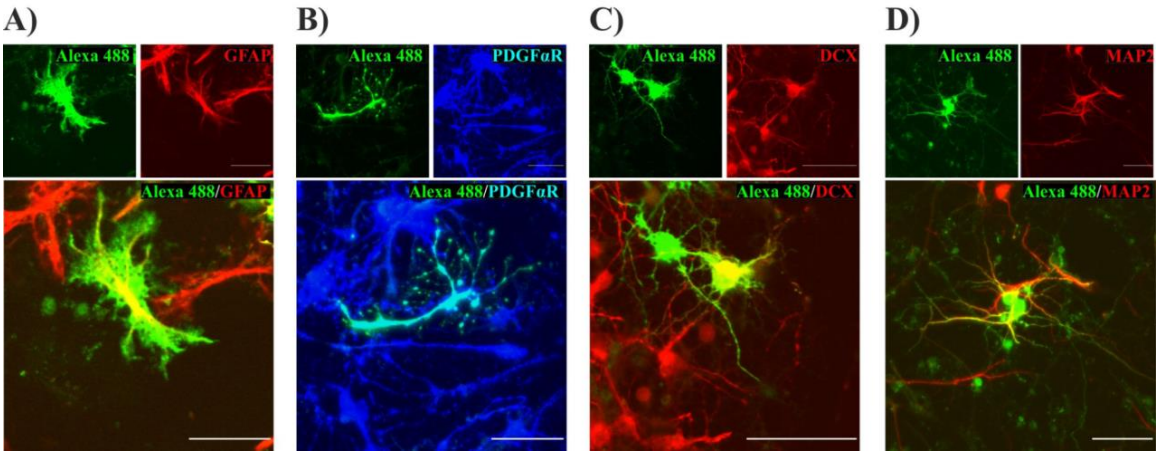

Figure 18: Immunocytochemistry of differentiated neural stem cells. A) Cells with a passive current pattern are mostly GFAP-positive and flat-shaped. **B)** Majority of cells displaying a complex current profile are branched or bipolar and PDGFαR-positive. **(C, D)** Cells with an outwardly rectifying current pattern are DCX/MAP2-positive, with round shape. Scale = 50 µm. **Abbreviations: DCX**= doublecortin; **GFAP**= glial fibrillary acidic protein; **MAP2**= microtubule associated protein 2; **PDGFαR**= platelet-derived growth – factor-α- receptor.

The electrophysiological analyses also revealed that Wnt signalling inhibition at the nuclear as well as membrane level markedly lowered the incidence of the cells displaying outwardly rectifying currents and raised the incidence of the cells with a passive current profile (Figure 19 and 20). On the other hand, activation of the pathway led to a decreased number of the cells with a passive current profile and to an increased number of the cells with an outwardly rectifying current pattern (Figure 21). Both, inhibition and activation of the pathway caused an increase in the incidence of cells displaying complex currents.

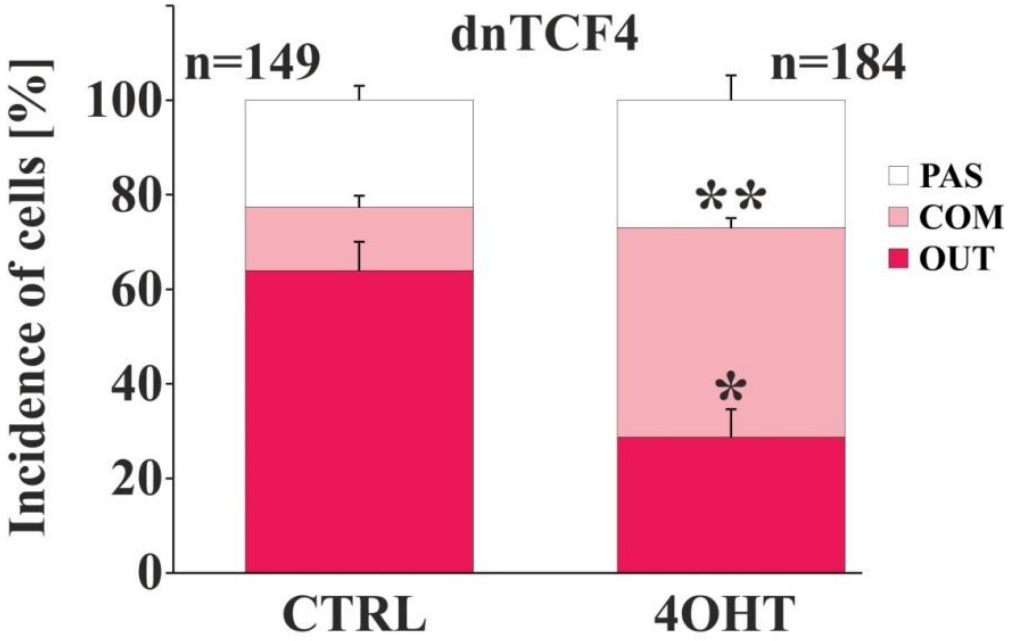

Figure 19: The incidence of the cells displaying passive (pas), complex (com) and outwardly (out) rectifying current profiles. These cells were derived from neonatal dnTCF4 nice. **Abbreviations: 4OHT**= tamoxifen-treated cultures; **CTRL**= control cultures.

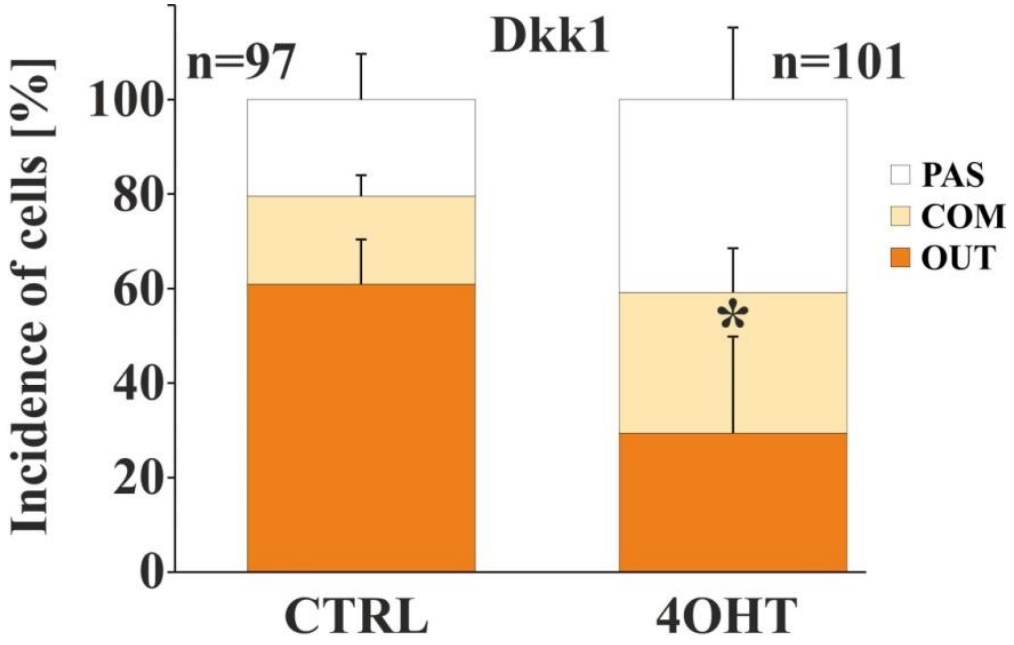

Figure 20: The incidence of the cells displaying passive (pas), complex (com) and outwardly (out) rectifying current profiles. These cells were derived from neonatal Dkk1 nice. **Abbreviations**: **4OHT**= tamoxifen-treated cultures; **CTRL**= control cultures.

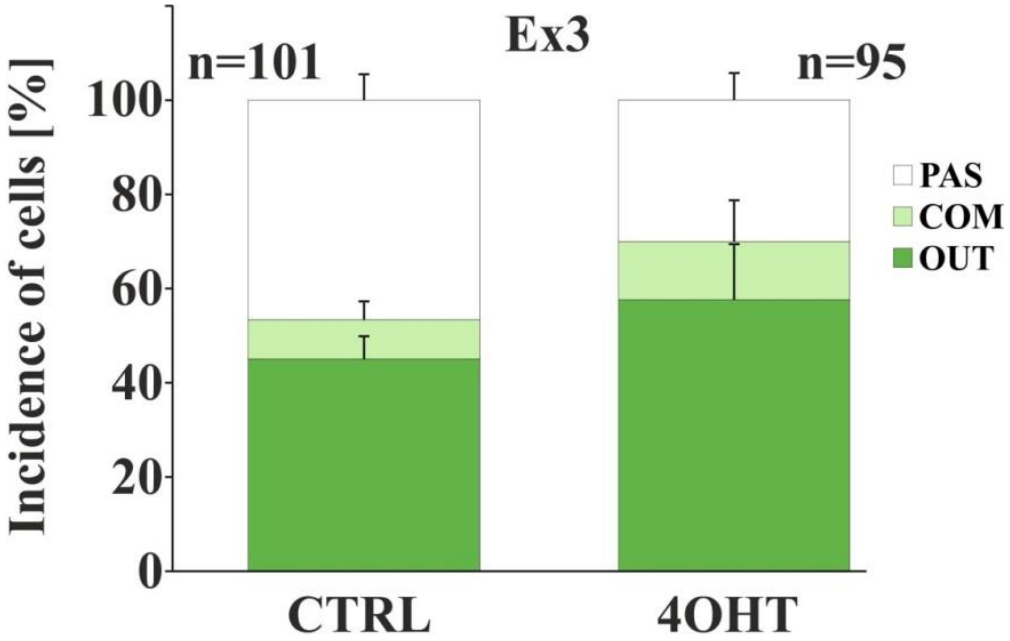

Figure 21: The incidence of the cells displaying passive (pas), complex (com) and outwardly (out) rectifying current profiles. These cells were derived from neonatal Ex3 nice. **Abbreviations**: **4OHT**= tamoxifen-treated cultures; **CTRL**= control cultures.

Next, we analyzed passive and active electrophysiological properties of differentiated NS/PCs (n=1245). Inhibition of the Wnt signaling pathway at the nuclear level (Table 2) and membrane level (Table 3) caused an increase in the membrane potential of the cells with a passive current pattern. The membrane capacitance was lower in the cells displaying complex and outwardly rectifying currents. The current densities of K_{IR} and K_{DR} currents were increased in the cells expressing complex and outwardly rectifying currents, respectively. The amplitude of K_A currents lowered in the cells displaying outwardly rectifying current patterns; however, K_A current density was not changed. Activation of the pathway (Table 4) led to the hyperpolarization of the membrane in the cells showing outwardly rectifying current profile and their input resistance was lowered. K_{IR} currents and their current densities were increased in the cells with a complex current pattern, while K_A currents or their current densities were markedly decreased in the cells displaying complex and outwardly rectifying current profile.

Table 2: Membrane properties of differentiated neonatal neural stem cells isolated from the frontal cortex of neonatal dnTcf4 mice. Abbreviations: dnTCF4= differentiated NS/PCs derived from neonatal dnTcf4 mice; **CTRL**= control; **4OHT**= 4-hydroxytamoxifen; **V_m,**= membrane potential; **IR**= input resistance; **C_m**= membrane capacitance; **K_{IR}**= inwardly rectifying K^+ current; **K_{DR}**= delayed outwardly rectifying K^+ current; **K_A**= fast activating and inactivating outwardly rectifying K^+ current; **K_{IR}/C_m, K_{DR}/C_m, K_A/C_m**= current densities; **n**= number of cells. Values in bold indicate significant differences between CTRL and 4OHT-treated cultures; **NS/PCs**= neural stem/progenitor cells. *, $p < 0.05$; **, $p < 0.01$; ***, $p < 0.001$

dnTcf4	**passive**		**complex**		**outwardly rectifying**	
properties	**CTRL**	**4OHT**	**CTRL**	**4OHT**	**CTRL**	**4OHT**
V_m [mV]c	**-83.3±0.6**	**-86.2±0.4*****	-83.6±1.3	-84.1±0.7	-69.1±1.3	-70.7±1.7
IR [MΩ]	73.6±3.1	73.2±2.3	202.9±18.0	214.2±11.4	1856.0±78.0	1817.7±98.8
C_m [pF]	34.4±2.2	31.3±1.6	**21.9±1.7**	**13.7±0.7*****	**10.6±0.4**	**7.5±0.3*****
K_{IR} [pA]	74.0±7.6	77.2±5.4	81.2±6.6	87.4±4.7	--	--
K_{IR}/C_m [pA/pF]	**2.3±0.2**	**3.9±0.3*****	**4.2±0.3**	**7.4±0.4*****	--	--
K_{DR} [pA]	127.0±17.1	119.4±11.4	514.9±44.2	463.0±29.4	691.0±23.5	637.3±26.0
K_{DR}/C_m [pA/pF]	3.8±0.5	4.3±0.4	**33.7±4.3**	**46.9±3.4***	**72.1±2.2**	**101.0±5.1*****
K_A [pA]	--	--	**290.3±35.5**	**205.0±12.4****	**634.5±27.5**	**479.2±27.7*****
K_A/C_m [pA/pF]	--	--	23.2±4.0	23.1±1.6	68.7±3.1	78.9±5.1
n	74	92	35	95	128	78

Table 3: Membrane properties of differentiated neonatal neural stem cells isolated from the frontal cortex of neonatal Dkk1 mice. Abbreviations: Dkk1= differentiated NS/PCs derived from neonatal Dkk1 mice; **CTRL**= control; **4OHT**= 4-hydroxytamoxifen; **V_m**= membrane potential; **IR**= input resistance; **C_m**= membrane capacitance; **K_{IR}**= inwardly rectifying K^+ current; **K_{DR}**= delayed outwardly rectifying K^+ current; **K_A**= fast activating and inactivating outwardly rectifying K^+ current; **K_{IR}/C_m, K_{DR}/C_m, K_A/C_m**= current densities; **n**= number of cells. Values in bold indicate significant differences between CTRL and 4OHT-treated cultures; **NS/PCs**= neural stem/progenitor cells. *, $p < 0.05$; **, $p < 0.01$; ***, $p < 0.001$

Dkk1	**passive**		**complex**		**outwardly rectifying**	
properties	**CTRL**	**4OHT**	**CTRL**	**4OHT**	**CTRL**	**4OHT**
V_m [mV]	**-85.2±0.4**	**-87.0±0.3*****	-85.2±0.9	-86.3±0.7	**-63.6±1.7**	**-74.9±2.9****
IR [MΩ]	71.2±2.3	71.6±1.8	**185.6±15.2**	**135.8±8.4****	1797.7±95.6	1514.3±181.8
C_m [pF]	**36.7±2.0**	**28.2±1.2*****	**22.4±1.2**	**16.7±0.8*****	**11.3±0.5**	**7.7±0.4*****
K_{IR} [pA]	58.0±4.6	56.3±3.3	**83.0±6.6**	**106.7±4.9****	--	--
K_{IR}/C_m [pA/pF]	2.3±0.2	2.7±0.2	**4.0±0.3**	**7.8±0.5*****	--	--
K_{DR} [pA]	82.3±9.1	78.6±8.1	**659.4±59.3**	**434.6±38.7****	830.1±34.6	881.1±79.0
K_{DR}/C_m [pA/pF]	3.2±0.3	3.9±0.5	38.0±4.4	38.3±4.2	**87.4±3.8**	**132.3±14.3*****
K_A [pA]	--	--	369.4±62.3	278.4±22.3	**795.1±38.5**	**524.0±49.5*****
K_A/C_m [pA/pF]	--	--	28.5±6.1	22.0±2.0	92.7±5.1	79.0±9.7
n	76	110	31	58	90	25

Table 4: Membrane properties of differentiated neonatal neural stem/progenitor cells isolated from the frontal cortex of neonatal Ex3 mice. Ex3= NS/PCs derived from neonatal Ex3 mice; **CTRL**= control; **4OHT**= 4-hydroxytamoxifen; **V_m**= membrane potential; **IR**= input resistance; **C_m**= membrane capacitance; **K_{IR}**= inwardly rectifying K^+ current; **K_{DR}**= delayed outwardly rectifying K^+ current; **K_A**= fast activating and inactivating outwardly rectifying K^+ current; **K_{IR}/C_m, K_{DR}/C_m, K_A/C_m**= current densities; **n**= number of cells. Values in bold indicate significant differences between CTRL and 4OHT-treated cultures; **NS/PCs**= neural stem/progenitor cells. *, $p < 0.05$; **, $p < 0.01$; ***, $p < 0.001$

Ex3	**passive**		**complex**		**outwardly rectifying**	
properties	**CTRL**	**4OHT**	**CTRL**	**4OHT**	**CTRL**	**4OHT**
V_m [mV]	**-85.7±0.3**	**-87.0±0.4****	-86.2±1.0	-87.5±0.7	**-67.0±2.1**	**-78.7±1.6*****
IR [MΩ]	**69.8±3.2**	**83.8±5.5***	**231.4±27.9**	**164.3±15.2***	**1924.7±82.1**	**1434.3±115.9*****
C_m [pF]	35.4±2.4	32.1±2.2	**17.4±1.8**	**23.5±1.8***	10.3±0.4	9.9±0.5
K_{IR} [pA]	71.4±6.1	86.7±6.5	**74.2±8.2**	**141.2±11.2*****	--	--
K_{IR}/C_m [pA/pF]	**2.7±0.2**	**4.2±0.3*****	**4.3±0.4**	**7.0±0.6****	--	--
K_{DR} [pA]	116.4±12.2	156.5±18.6	618.5±61.2	605.8±40.9	652.7±25.3	695.6±42.1
K_{DR}/C_m [pA/pF]	4.1±0.4	5.3±0.6	43.3±4.4	36.0±3.5	71.2±3.1	75.9±3.6
K_A [pA]	--	--	229.8±24.0	275.6±38.3	**675.9±37.6**	**441.8±37.1*****
K_A/C_m [pA/pF]	--	--	20.5±3.5	13.4±1.6	**80.3±5.2**	**55.9±5.0****
n	89	65	19	40	77	63

Furthermore, we identified changes in current densities of voltage-dependent Na^+ channels in DCX/MAP2-positive cells, with an outwardly rectifying current pattern (Figure 22A), and also the changes in the incidence of such cells (Figure 22B) that were also capable of generating action potentials (Figure 22C). Inhibition at the membrane and nuclear level led to the absence of cells expressing Na^+ channels, while activation of the pathway caused an increase in the Na^+ current densities as well as in the cell incidence.

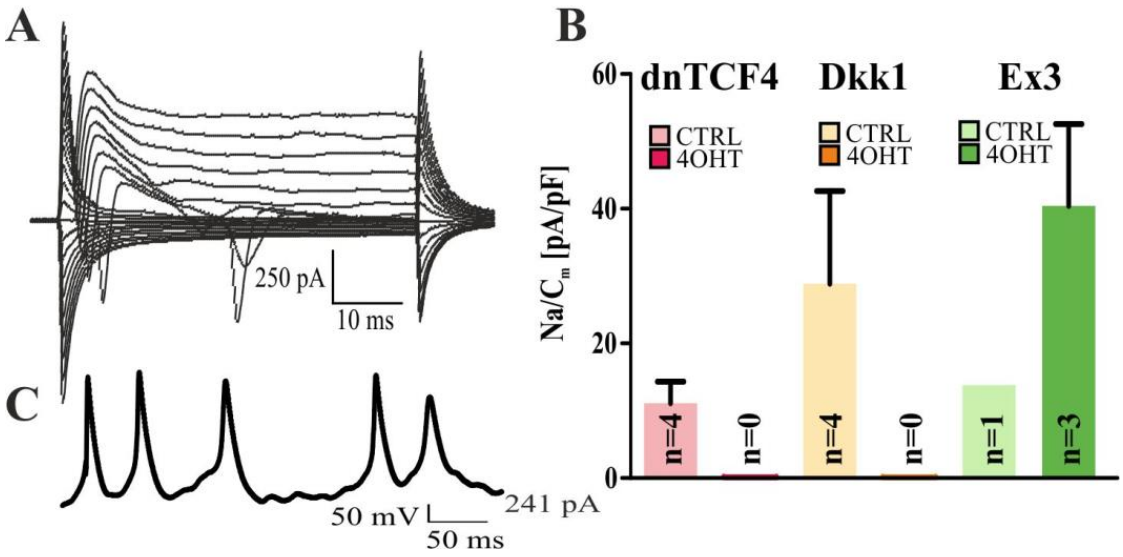

Figure 22: Voltage-dependent Na^+ channels in the cells with an outwardly rectifying current profile. A) A typical current pattern of a cell expressing outwardly rectifying K^+ currents along with inwardly rectifying Na^+ currents. **B)** Some of the cells are capable of generating action potentials; the trace represents such action potentials. **(C)** Inhibiting Wnt signalling at the nuclear (dnTcf4) and membrane (Dkk1) level causes a decrease in the incidence of cells expressing Na^+ channels. In contrast, activating the pathway (Ex3) leads to an increase in the incidence as well as in the current density of voltage-gated Na^+ channels. **Abbreviations: dnTcf4**= differentiated neural stem/progenitor cells derived from neonatal dnTcf4 mice; **Dkk1**= differentiated neural stem/progenitor cells derived from neonatal Dkk1 mice; **Ex3**= differentiated neural stem/progenitor cells derived from neonatal Ex3 mice; **CTRL**= control cultures; **4OHT**= tamoxifen-treated cultures; **n**= number of cells; **Na/C_m**= current density of Na^+ currents; **Wnt**= Wingless/Integrated.

4.2 Adult neural stem/progenitor cells

4.2.1 Beta-catenin levels in differentiated adult neural stem/progenitor cells

We also carried out immunocytochemical analyses of β-catenin in differentiated adult NS/PCs (Figure 23 and 24). Our results were same as in immunocytochemical analyses of differentiated neonatal NS/PCs. So, after inhibiting the Wnt/β-catenin signalling pathway in the nucleus (dnTCF4; Figure 23A and 24), there were no changes in the expression of the β-catenin. Inhibiting Wnt signalling pathway at the cell membrane level (Dkk1; Figure 23B and 24) resulted in a marked decrease in the protein expression and activation of the Wnt signalling pathway (Ex3; Figure 23C and 24) led to an increase in the β-catenin protein in the cytoplasm.

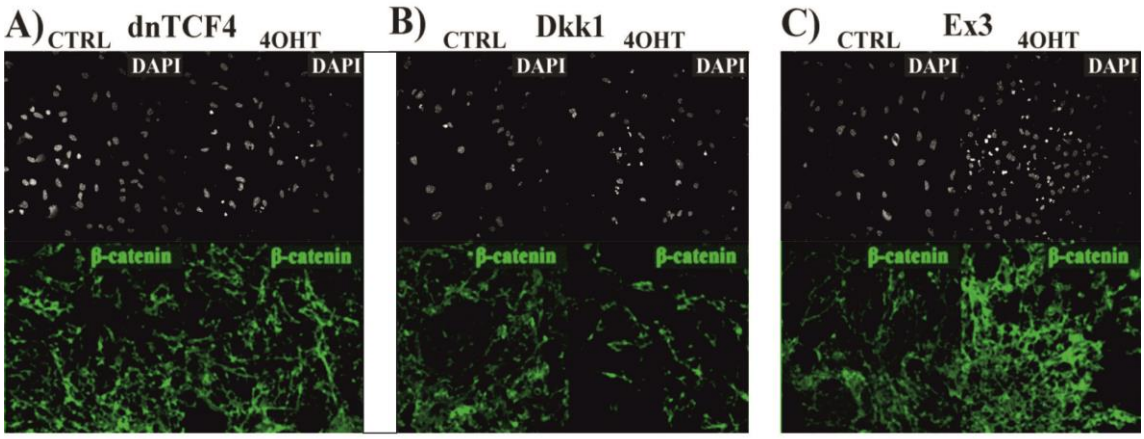

Figure 23: Beta-catenin staining in differentiated adult neural stem cells: A) Fluorescent images of β-catenin staining in differentiated NS/PCs derived from adult dnTCF4 mice with inhibited Wnt signalling pathway at the nuclear level in CTRL and 4OHT cultures. **B)** Fluorescent images of β-catenin staining in differentiated NS/PCs derived from adult Dkk1 mice with inhibited Wnt signalling pathway at the membrane level in CTRL and 4OHT cultures. **C)** Fluorescent images of β-catenin staining in differentiated NS/PCs derived from adult Ex3 mice with activated Wnt signalling pathway in the cytoplasm in CTRL and 4OHT cultures. **Abbreviations**: **4OHT**= tamoxifen-treated cultures; **CTRL**= control cultures; **DAPI**= 4',6-diamidino-2-phenylindole; **Dkk1**= NS/PCs derived from adultl Dkk1 mice; **dnTCF4**= NS/PCs derived from adult dnTCF4 mice; **Ex3**= NS/PCs derived from adult Ex3 mice; **NS/PCs**= neural stem/progenitor cells; **Wnt**= Wingless/Integrated.

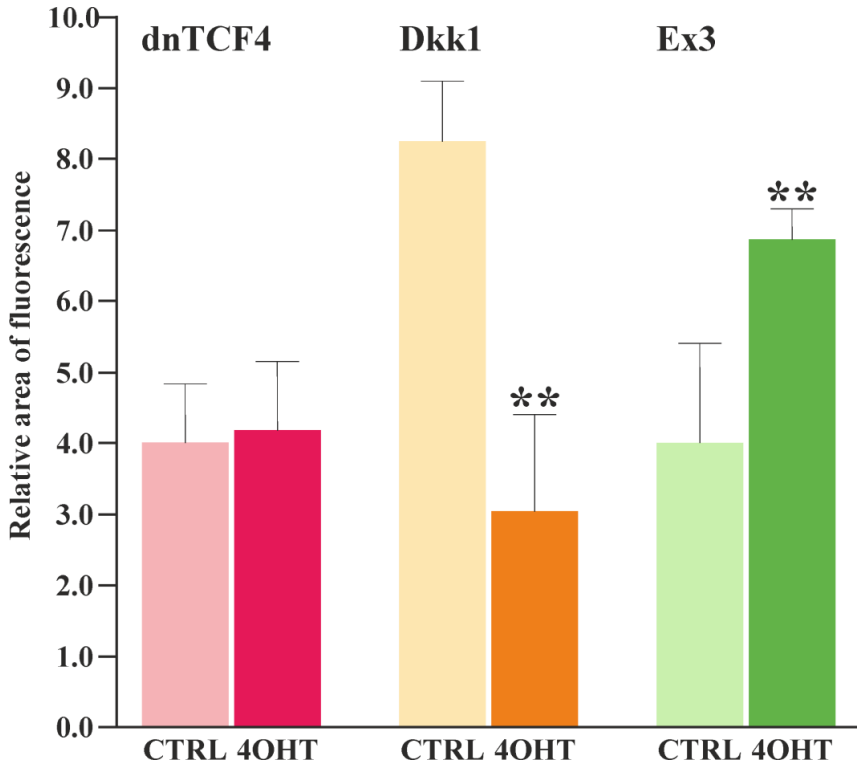

Figure 24: Quantification of β-catenin expression showing the proportion of area of positively-stained cells to DAPI-positive area (n=12). The values are represented as mean ± S.D. Statistical significance was calculated using t-test. ** $p < 0.01$. Note similar changes in β-catenin levels in response to Wnt signalling inhibition/activation in differentiated adult NS/PCs. **Abbreviations**: **4OHT**= tamoxifen-treated cultures; **CTRL**= control cultures; **Dkk1**= NS/PCs derived from adult Dkk1 mice; **dnTCF4**= NS/PCs derived from adult dnTCF4 mice; **Ex3**= NS/PCs derived from adult Ex3 mice.

4.2.2 Membrane properties of differentiated adult neural stem/progenitor cells

Similarly adult control (n=413) and 4OHT-treated (n=452) cells were again divided into three groups according to their electrophysiological properties:

a) Cells displaying passive time- and voltage-independent K^+ currents (passive current profile; n=261) were characterized by average V_m of -86.38 ± 0.26 mV and IR of 81.62 ± 1.91 MΩ.

b) Cells showing an outwardly rectifying current pattern (n=262) were characterized by V_m of -72.04 ± 0.90 mV and high values of IR (1649.79 ± 44.05 MΩ).

c) Cells with a complex current pattern (n=342) had V_m of -85.78 ± 0.45 mV and IR of 218.56 ± 8.24 MΩ.

Interestingly, Wnt signalling inhibition/activation had no impact on the incidence of three distinct current profiles in differentiated NS/PCs derived from al three mouse strains (Figures 25, 26, 27).

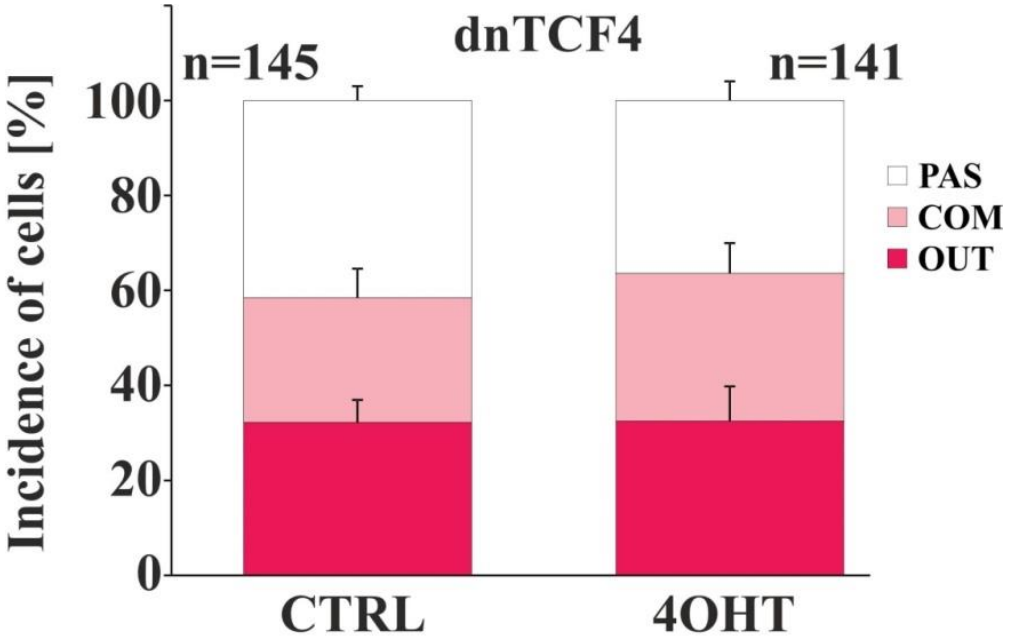

Figure 25: The incidence of the cells displaying passive, complex and outwardly rectifying current profiles. These cells were isolated from adult dnTCF4 mice. **Abbreviations: 4OHT**= tamoxifen-treated cultures; **CTRL**= control cultures.

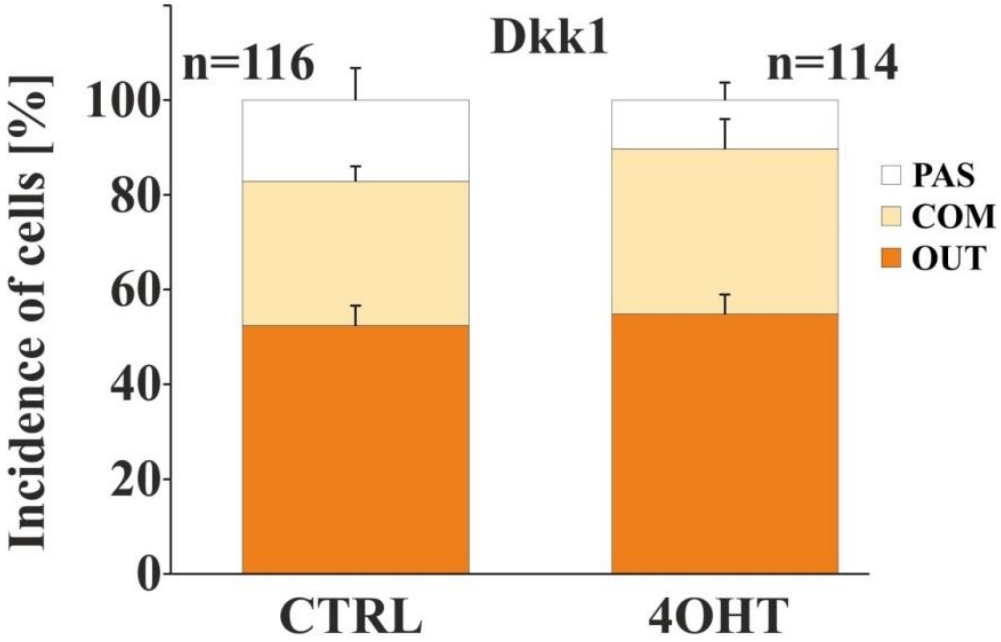

Figure 26: The incidence of the cells displaying passive, complex and outwardly rectifying current profiles. These cells were isolated from adult Dkk1 mice. **Abbreviations: 4OHT**= tamoxifen-treated cultures; **CTRL**= control cultures.

7

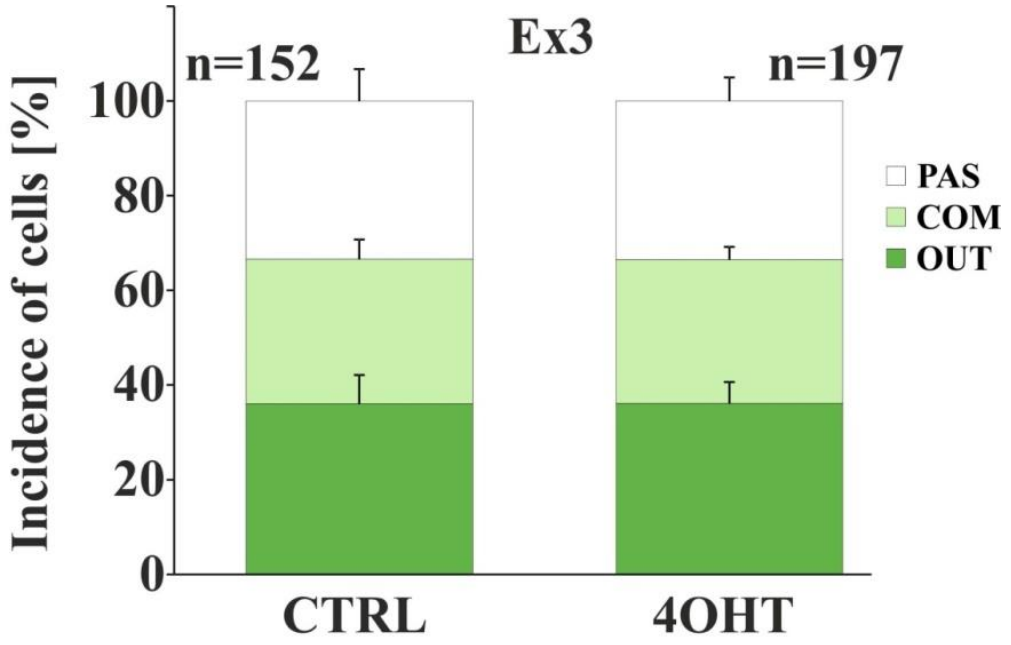

Figure 27: The incidence of the cells displaying passive, complex and outwardly rectifying current profiles. These cells were isolated from adult Ex3 mice. Abbreviations: **4OHT**= tamoxifen-treated cultures; **CTRL**= control cultures.

Additionaly, we analyzed passive and active electrophysiological properties of 901 differentiated cells, which were isolated from adult Dkk1, dnTCF4 and Ex3 mice.

When compared to controls, inhibition of Wnt/β-catenin signaling pathway at the nuclear (dnTCF4) caused an increase in the V_m in cells with complex current pattern and V_m decrease in cells displaying outwardly rectifying current pattern. The C_m decreased in the cells displaying passive current pattern. The current densities of K_{DR} currents were significantly increased in the cells expressing outwardly rectifying current pattern (Table 5).

Inhibition of this pathway at the membrane level (Dkk1) caused a significant decrease in the V_m of the cells with outwardly rectifying currents. Compared to controls the C_m was lower in the cells displaying passive current pattern but higher in the cells displaying outwardly rectifying currents. The current densities of K_{DR} currents was increased in cells with complex and outwardly rectifying current but current density of K_A currents were decreased (Table 6).

Activation of Wnt/β-catenin signaling pathway led to the hyperpolarization of the cell membrane in the cells expressing outwardly rectifying currents and their input resistance was lowered. K_{IR} currents and their current densities were significant decreased in the cells with a complex current pattern, same as K_A currents (Table 7).

Table 5: Membrane properties of differentiated adult neural stem cells isolated from SVZ of adult dnTcf4 mice. Abbreviations: dnTCF4= differentiated NS/PCs derived from adult dnTcf4 mice; **CTRL**= control; **4OHT**= 4-hydroxytamoxifen; **V_m**,= membrane potential; **IR**= input resistance; **C_m**= membrane capacitance; **K_{IR}**= inwardly rectifying K^+ current; **K_{DR}**= delayed outwardly rectifying K^+ current; **K_A**= fast activating and inactivating outwardly rectifying K^+ current; **K_{IR}/C_m, K_{DR}/C_m, K_A/C_m**= current densities; **n**= number of cells. Values in bold indicate significant differences between CTRL and 4OHT-treated cultures; **SVZ**= subventricular zone; **NS/PCs**= neural stem/progenitor cells. *, $p < 0.05$; **, $p < 0.01$; ***, $p < 0.001$

dnTcf4	**passive**		**complex**		**outwardly rectifying**	
properties	**CTRL**	**4OHT**	**CTRL**	**4OHT**	**CTRL**	**4OHT**
V_m [mV]	-84.5±0.5	-83.0±0.6	**-82.9±0.9**	**-88.7±0.5*****	**-85.5±1.1**	**-79.4±1.4*****
IR [MΩ]	67.6±3.06	66.7±2.4	138.2±9.6	151.0±9.5	977.1±77.7	934.6±78.8
C_m [pF]	27.1±1.6	30.4±1.7	**16.9±1.0**	**12.8±0.7****	8.4±0.4	9.5±0.5
K_{IR} [pA]	59.4±4.2	56.1±4.7	90.5±6.9	86.6±7.3	--	--
K_{IR}/C_m [pA/pF]	2.9 ±0.2	2.5±0.3	6.4±0.5	7.8±0.7	--	--
K_{DR} [pA]	**70.4±12.4**	**122.4±17.9***	489.7±53.1	517.0±45.2	**816.5±30.7**	**1024.3±58.5****
K_{DR}/C_m [pA/pF]	**3.7±0.6**	**6.1±0.4***	**34.9±3.8**	**52.2±5.7***	112.2±2.2	118.3±6.3
K_A [pA]	--	--	**331.9±46.6**	**200.4±15.9****	605.7±41.0	489.7±45.3
K_A/C_m [pA/pF]	--	--	22.3±3.3	20.8±2.5	84.5±5.6	75.5±8.3
n	62	55	43	46	47	47

Table 6: Membrane properties of differentiated adult neural stem cells isolated from the SVZ of adult Dkk1 mice. Abbreviations: Dkk1= differentiated NS/PCs derived from adult Dkk1 mice; **CTRL**= control; **4OHT**= 4-hydroxytamoxifen; **V_m**= membrane potential; **IR**= input resistance; **C_m**= membrane capacitance; **K_{IR}**= inwardly rectifying K^+ current; **K_{DR}**= delayed outwardly rectifying K^+ current; **K_A**= fast activating and inactivating outwardly rectifying K^+ current; **K_{IR}/C_m, K_{DR}/C_m, K_A/C_m**= current densities; **n**= number of cells. Values in bold indicate significant differences between CTRL and 4OHT-treated cultures; **SVZ**= subventricular zone; **NS/PCs**= neural stem/progenitor cells. *, $p < 0.05$; **, $p < 0.01$; ***, $p < 0.001$

Dkk1	**passive**		**complex**		**outwardly rectifying**	
properties	**CTRL**	**4OHT**	**CTRL**	**4OHT**	**CTRL**	**4OHT**
V_m [mV]	-86.8±0.6	-85.5±0.7	**-89.0±0.7**	**-86.9±0.7***	**-86.9±0.9**	**-81.8±1.0*****
IR [MΩ]	**49.1±2.4**	**75.3±1.8*****	136.4±7.7	136.3±6.9	**1020.0±92.7**	**352.4±22.3*****
C_m [pF]	**31.4±2.2**	**21.7±1.4*****	14.5±0.8	15.2±1.1	**9.1±0.4**	**16.1±1.0*****
K_{IR} [pA]	62.2±9.4	63.9±6.9	109.5±7.4	119.4±8.5	--	--
K_{IR}/C_m [pA/pF]	2.4±0.4	3.2±0.3	8.5±0.6	10.7±1.0	--	--
K_{DR} [pA]	166.2±25.0	144.0±22.8	708.2±65.4	881.1±60	**1149.3±51.1**	**1656.5±62.4*****
K_{DR}/C_m [pA/pF]	7.4±1.5	8.7±1.7	**54.1±5.0**	**76.0±7.3***	139.6±6.6	150.5±11.9
K_A [pA]	--	--	**507.2±50.3**	**302.4±19.8****	**859.7±50.0**	**352.1±31.1*****
K_A/C_m [pA/pF]	--	--	**45.4±4.9**	**25.1±2.1****	**110.9±8.0**	**40.1±6.0*****
n	25	25	39	38	65	57

Table 7: Membrane properties of differentiated adult neural stem cells isolated from the SVZ of adult Ex3 mice. Abbreviations: Ex3= differentiated NS/PCs derived from adult Ex3 mice; **CTRL**= control; **4OHT**= 4-hydroxytamoxifen; $\mathbf{V_m}$= membrane potential; **IR**= input resistance; $\mathbf{C_m}$= membrane capacitance; $\mathbf{K_{IR}}$= inwardly rectifying K^+ current; $\mathbf{K_{DR}}$= delayed outwardly rectifying K^+ current; $\mathbf{K_A}$= fast activating and inactivating outwardly rectifying K^+ current**;** $\mathbf{K_{IR}/C_m}$, $\mathbf{K_{DR}/C_m}$, $\mathbf{K_A/C_m}$= current densities; **n**= number of cells. Values in bold indicate significant differences between CTRL and 4OHT-treated cultures; **SVZ**= subventricular zone; **NS/PCs**= neural stem/progenitor cells. *, $p < 0.05$; **, $p < 0.01$; ***, $p < 0.001$

Ex3	**passive**		**complex**		**outwardly rectifying**	
properties	**CTRL**	**4OHT**	**CTRL**	**4OHT**	**CTRL**	**4OHT**
V_m [mV]	**-85.4±0.4**	**-87.6±0.4*****	**-88.8±0.6**	**-86.5±0.5****	**-86.2±1.1**	**-77.8±1.5*****
IR [MΩ]	**89.4±3.7**	**79.2±3.1***	**175.6±11.2**	**139.4±6.1****	**1304.2±120.6**	**913.5±74.6****
C_m [pF]	22.6±1.2	20.7±1.1	15.7±0.9	17.1±0.9	**9.1±0.4**	**11.1±0.6****
K_{IR} [pA]	57.0±5.9	45.8±3.2	**105.4±6.8**	**64.0±4.8*****	--	--
K_{IR}/C_m [pA/pF]	3.5±0.4	2.7±0.2	**7.9±0.5**	**4.7±0.4*****	--	--
K_{DR} [pA]	**116.7±11,8**	**72.6±9.3****	**545.4±46.5**	**383.9±26.6****	853.5±37.4	852.9.±42.0
K_{DR}/C_m [pA/pF]	**5.8±0.6**	**3.8±0.5***	**42.1±3.7**	**25.5±1.9*****	**101.2±4.0**	**88.5±4.6***
K_A [pA]	--	--	**253.9±40.7**	**148.0±19.5***	**675.9±37.6**	**320.4±29.8*****
K_A/C_m [pA/pF]	--	--	**19.2±3.2**	**11.2±1.7***	**80.6±5.9**	**44.0±5.1*****
n	61	63	45	59	62	62

5 DISCUSSION

In the present study, we introduced three transgenic mouse strains (dnTCF4, Dkk1, Ex3) utilizing the Cre-loxP system. These transgenic mouse strains might represent suitable animal models for manipulating the canonical, Wnt/β-catenin pathway at different subcellular levels, and subsequently affecting neurogenesis and gliogenesis in neonatal and adult mice *in vitro*.

We demonstrated that blocking of this signalling pathway in NS/PCs isolated from neonatal Dkk1 mice, resulted in decreased amounts of β-catenin, while its stabilization was detected in Ex3 cells producing a truncated variant of the protein. Moreover, activation of Wnt/β-catenin signalling pathway increased the expression of β III tubulin and decreased the incidence of GFAP-positive cells displaying passive current profile. On the contrary, by supressing the Wnt signalling pathway, the incidence of GFAP positive cells increased and number of DCX/MAP2 positive cells expressing outwardly rectifying current profile decreased. Furthermore, Wnt signaling activation increased the incidence of cells expressing outwardly rectifying K^+ currents together with inwardly rectifying Na^+ currents.

However, after activation or inhibition Wnt signalling in differentiated NS/PCs isolated from adult dnTCF4, Dkk1, and Ex3 mice we found no differences in the incidence of three current profiles.

5.1 Impact of Wnt signalling activation/inhibition on beta-catenin levels in differentiated neural stem/progenitor cells

Based on the findings from *in vitro* studies disclosing an impact of Wnt signalling on stem cells differentiation (Prajerova et al., 2010), we employed three transgenic mouse strains enabling tamoxifen-induced Cre-mediated DNA recombination: dnTCF4, Dkk1 and Ex3 strain. In the mouse strain dnTCF4, we were able to inhibit Wnt signalling pathway at the nuclear level, while in the Dkk1 mouse we inhibited Wnt cascade at the membrane level. Conversely, in the mouse strain Ex3 we were able to activate Wnt signalling pathway through the production of a stable form of β-catenin protein.

In contrast to our study, other authors opted for different approaches to study the effect of canonical Wnt signalling pathway on neonatal and adult stem cells differentiation *in vitro*. Hirsch and co-workers (2007) added recombinant Wnt3a to the differentiation media of NS/PCs isolated during the neurogenic phase from the mouse cerebral cortex, Lie and

colleagues (2005) in their study demonstrated, that overexpression of Wnt3 was sufficient to increase neurogenesis in adult hippocampal stem cells isolated from the rat brain or another group used NS/PCs transduced with Wnt-7a (Prajerova et al., 2010).

It is worth mentioning that we obtained similar results as the above-mentioned authors since we found that in our mice, Wnt signalling manipulation led to changes in the expression of β-catenin levels and Wnt signalling target genes (data not shown). Conversely, inhibition of the pathway in the dnTcf4 mouse did not affect the levels of β-catenin expression, which accords well with the fact that the alteration in the pathway occurs in the nucleus – downstream of β-catenin production, whereas this was not the case in Dkk1 and Ex3 mice, where the alterations occurred at the membrane and the protein itself, respectively.

5.2 Wnt signalling promotes differentiation of neonatal neural progenitors towards neuron-like cells

Our *in vitro* data obtained from three transgenic mouse models revealed that canonical Wnt signalling pathway increases the incidence of cells positive for neuronal marker β III tubulin and decreases the incidence of GFAP-positive cells, thus promoting neurogenesis and supressing gliogenesis, only in neonatal mice. Despite the fact that changes in β-catenin levels in response to Wnt signalling manipulation were comparable in both neonatal and adult NS/PCs, in differentiated cultures of adult NS/PCs, we did not observed any changes in the incidence of cells positive for neuronal marker β III tubulin and also GFAP-positive cells. This is an interesting finding, which might point towards other regulatory mechanisms that are present in adult brain and limit/alter the functioning of Wnt signalling pathway.

Hirsch and colleagues (2007) demonstrated similar effects of Wnt signalling on the expression of β III tubulin, although the number of GFAP-positive cells remained unchanged. It is obvious that such discrepancies might stream from the presence of different Wnt ligands. We exposed our NS/PCs cultures to the mixture of Wnt signals, whereas they applied specifically only Wnt3 ligand. Furthermore, we observed that Wnt signalling causes higher incidence of DCX/MAP2-positive cells concomitantly with the fact that these cells were more developed (more branched processes), which is in concordance with previously published data from *in vitro* experiments (Kunke et al.,

2009). They transduced mouse NS/PCs with constructs producing Wnt7a or Dkk1 and showed that these molecules influenced the cell fate during differentiation. The expression of Wnt7a (Wnt signalling activation) led to an increase in the incidence of MAP2-positive cells, while GFAP-positive cells were suppressed. In contrast, Dkk1 (Wnt signalling inhibition) significantly increased gliogenesis at the expense of neurogenesis.

Therefore, we concluded that Wnt signalling has a crucial role in the control of neuronal progenitor differentiation postnatally, while the functioning of Wnt signalling pathway in the SVZ of the adult mouse brain is altered/compromised.

5.3 Wnt signalling has an impact on electrophysiological properties of differentiated neonatal NS/PCs *in vitro*

Previously, it was shown that overexpressing Wnt-7a electrophysiological properties of differentiated neural precursors (Prajerova et al., 2010). Wnt signalling caused higher incidence of cells expressing outwardly rectifying K^+ currents, TTX-sensitive inwardly rectifying Na^+ currents, and generating action potentials. This neuron-like current pattern also prevailed in our experiments. In our work, we further disclose that MAP2-positive cells displayed large K_A and K_{DR} current amplitudes, which corroborates previous studies in neonatal NS/PCs transduced with Wnt7a (Prajerova et al., 2010). Concomitantly, in differentiated NS/PCs derived from mice with inhibited Wnt signalling, we found that the response of MAP2/DCX-positive cells to glutamate application decreased. These data, obtained from calcium imaging, support the presence of glutamate receptors on neural progenitors; glutamate receptors mediate excitation-induced neurogenesis by inhibiting the expression of the glial transcription factors Hes1 and Id2, and by promoting expression of the pro-neuronal transcription factor NeuroD, as suggested by (Deisseroth et al., 2004). Using retrovirus-mediated gene knock-out in mice, (Tashiro et al., 2006) showed that the survival of maturating neurons is competitively regulated by their own NMDA receptors during a short period after neuronal birth. Next, we found that inhibition of the Wnt pathway led to increased number of cells responding to the ATP application, nevertheless, elevated β-catenin signalling resulted in the lower average response amplitude. This is in the contrast with the *in vitro* observations that ATP up-regulates the Tuj1, NeuN (neuronal markers) and β-catenin expression and thus promotes the neuronal differentiation of stem cells (Tu et al., 2014). Here, we might find the reason of this discrepancy in using different

cells; we used neural stem cells, while (Tu et al., 2014) employed mesenchymal stem cells in their study.

In summary, the Wnt signalling pathway regulates neurogenesis as it drives the neonatal NS/PCs differentiation into the DCX/MAP2-positive cells expressing outwardly rectifying K^+ currents and inwardly rectifying Na^+ currents. Importantly, we believe that manipulating β-catenin signalling in neonatal NS/PCs may provide new approaches to cure the diseased CNS. For instance, studies of progenitor cells in the olfactory epithelium of neonatal and adult mice *in vivo* suggested a key role of Wnt signalling in maintaining progenitor cells proliferation under normal conditions and promoting neuroregeneration after epithelial lesion (Chen et al., 2014). Moreover, a strong relationship between Alzheimer's disease and Wnt signalling pathway impairments has been suggested (Inestrosa et al., 2002).

Based on above mentioned findings, we will further focus on Wnt signalling in adult brain during CNS disorders, such as ischemic injury or Alzheimer disease to test the differentiation potential of adult NS/PCs isolated from injured brains.

6 CONCLUSIONS

In this study we employed transgenic mice that serve as a suitable animal model for manipulating canonical Wnt signaling. Furthermore, we demonstrated that Wnt signaling in cell cultures derived from neonatal mice increase the number of DCX/MAP2/β III tubulin-positive cells, yet on the other hand, decrease the counts of GFAP-positive cells. Hyperactive Wnt/β-catenin signaling also increased the incidence of cells displaying an outwardly rectifying K^+ current profile together with inwardly rectifying Na^+ currents. Our data indicate that the Wnt signaling pathway in a newborn mouse brain regulates the NS/PCs differentiation towards cells with features of neuroblasts or immature neurons (Figure 28).

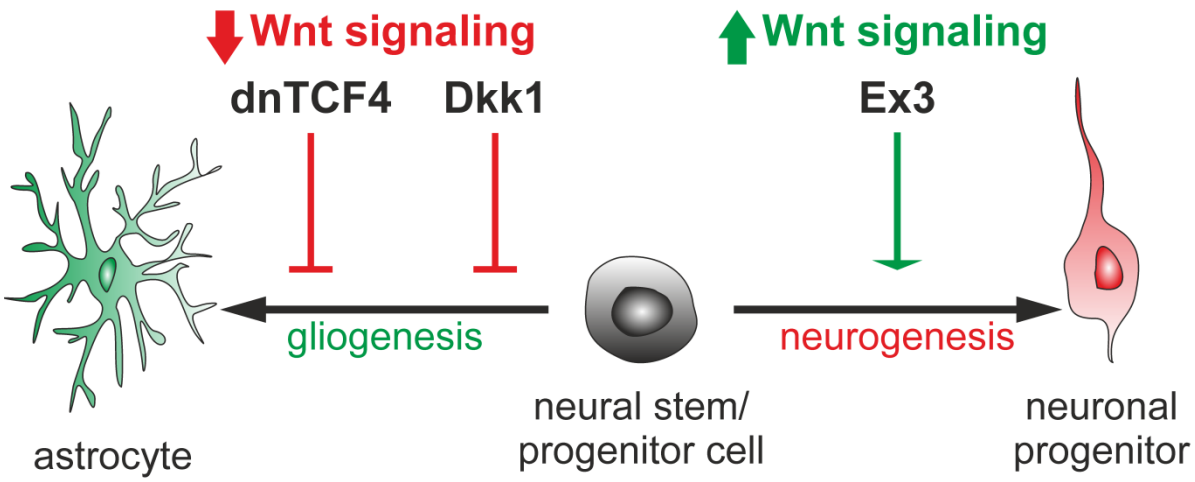

Figure 28: Graphical summary of our results. Inhibition of the Wnt signalling in neonatal NS/PCs (dnTCF4 and Dkk1 mouse strains) promoted gliogenesis at the expense of neurogenesis. On the other hand, Wnt signalling activation resulted in the opposite effect – in Ex3 cultures, neurogenesis was increased and gliogenesis decreased. **Abbreviations: Dkk1**= neural stem /progenitor cells derived from neonatal Dkk1 mice; **dnTCF4**= neural stem/progenitor cells derived from adult dnTCF4 mice; **Ex3**= neural stem/progenitor cells derived from adult Ex3 mice; **Wnt**= Wingless/Integrated; NS/PCs= neural stem/progenitor cells.

7 REERENCES

Adachi K, Mirzadeh Z, Sakaguchi M, Yamashita T, Nikolcheva T, Gotoh Y, Peltz G, Gong L, Kawase T, Alvarez-Buylla A, Okano H, Sawamoto K (2007) Beta-catenin signaling promotes proliferation of progenitor cells in the adult mouse subventricular zone. Stem Cells 25:2827-2836.

Aimone JB, Li Y, Lee SW, Clemenson GD, Deng W, Gage FH (2014) Regulation and Function of Adult Neurogenesis: From Genes to Cognition. Physiol Rev 94:991-1026.

Altman J, Das GD (1965) Autoradiographic and histological evidence of postnatal hippocampal neurogenesis in rats. J Comp Neurol 124:319-335.

Anderova M, Vorisek I, Pivonkova H, Benesova J, Vargova L, Cicanic M, Chvatal A, Sykova E (2011) Cell death/proliferation and alterations in glial morphology contribute to changes in diffusivity in the rat hippocampus after hypoxia-ischemia. J Cereb Blood Flow Metab 31:894-907.

Anderová M, Kubinová S, Jelitai M, Neprasová H, Glogarová K, Prajerová I, Urdzíková L, Chvátal A, Syková E (2006) Transplantation of embryonic neuroectodermal progenitor cells into the site of a photochemical lesion: immunohistochemical and electrophysiological analysis. J Neurobiol 66:1084-1100.

Apte MV, Haber PS, Applegate TL, Norton ID, McCaughan GW, Korsten MA, Pirola RC, Wilson JS (1998) Periacinar stellate shaped cells in rat pancreas: identification, isolation, and culture. Gut 43:128-133.

Axelrod JD, Miller JR, Shulman JM, Moon RT, Perrimon N (1998) Differential recruitment of Dishevelled provides signaling specificity in the planar cell polarity and Wingless signaling pathways. Genes Dev 12:2610-2622.

Bean BP (2007) The action potential in mammalian central neurons. Nat Rev Neurosci 8:451-465.

Bovolenta P, Esteve P, Ruiz JM, Cisneros E, Lopez-Rios J (2008) Beyond Wnt inhibition: new functions of secreted Frizzled-related proteins in development and disease. J Cell Sci 121:737-746.

Briscoe J, Novitch BG (2008) Regulatory pathways linking progenitor patterning, cell fates and neurogenesis in the ventral neural tube. Philos Trans R Soc Lond B Biol Sci 363:57-70.

Brown JP, Couillard-Després S, Cooper-Kuhn CM, Winkler J, Aigner L, Kuhn HG (2003) Transient expression of doublecortin during adult neurogenesis. J Comp Neurol 467:1-10.

Cameron HA, McKay RD (2001) Adult neurogenesis produces a large pool of new granule cells in the dentate gyrus. J Comp Neurol 435:406-417.

Chen M, Tian S, Yang X, Lane AP, Reed RR, Liu H (2014) Wnt-responsive Lgr5^{+} globose basal cells function as multipotent olfactory epithelium progenitor cells. J Neurosci 34:8268-8276.

Chvátal A, Anderová M, Ziak D, Syková E (1999) Glial depolarization evokes a larger potassium accumulation around oligodendrocytes than around astrocytes in gray matter of rat spinal cord slices. J Neurosci Res 56:493-505.

Cisternas P, Henriquez JP, Brandan E, Inestrosa NC (2014) Wnt signaling in skeletal muscle dynamics: myogenesis, neuromuscular synapse and fibrosis. Mol Neurobiol 49:574-589.

Cocchia D, Michetti F, Donato R (1981) Immunochemical and immuno-cytochemical localization of S-100 antigen in normal human skin. Nature 294:85-87.

Cruciat CM, Niehrs C (2013) Secreted and transmembrane wnt inhibitors and activators. Cold Spring Harb Perspect Biol 5:a015081.

Deisseroth K, Singla S, Toda H, Monje M, Palmer TD, Malenka RC (2004) Excitation-neurogenesis coupling in adult neural stem/progenitor cells. Neuron 42:535-552.

Doetsch F (2003) The glial identity of neural stem cells. Nat Neurosci 6:1127-1134.

Doetsch F, Caillé I, Lim DA, García-Verdugo JM, Alvarez-Buylla A (1999) Subventricular zone astrocytes are neural stem cells in the adult mammalian brain. Cell 97:703-716.

Doubravska L, Krausova M, Gradl D, Vojtechova M, Tumova L, Lukas J, Valenta T, Pospichalova V, Fafilek B, Plachy J, Sebesta O, Korinek V (2011) Fatty acid modification of Wnt1 and Wnt3a at serine is prerequisite for lipidation at cysteine and is essential for Wnt signalling. Cell Signal 23:837-848.

Eng LF, Ghirnikar RS, Lee YL (2000) Glial fibrillary acidic protein: GFAP-thirty-one years (1969-2000). Neurochem Res 25:1439-1451.

Fuentealba LC, Obernier K, Alvarez-Buylla A (2012) Adult neural stem cells bridge their niche. Cell Stem Cell 10:698-708.

Goel M, Dhingra NK (2012) Müller glia express rhodopsin in a mouse model of inherited retinal degeneration. Neuroscience 225:152-161.

Graham TA, Weaver C, Mao F, Kimelman D, Xu W (2000) Crystal structure of a beta-catenin/Tcf complex. Cell 103:885-896.

Guérette D, Khan PA, Savard PE, Vincent M (2007) Molecular evolution of type VI intermediate filament proteins. BMC Evol Biol 7:164.

Harada N, Tamai Y, Ishikawa T, Sauer B, Takaku K, Oshima M, Taketo MM (1999) Intestinal polyposis in mice with a dominant stable mutation of the beta-catenin gene. EMBO J 18:5931-5942.

Hsieh JC, Kodjabachian L, Rebbert ML, Rattner A, Smallwood PM, Samos CH, Nusse R, Dawid IB, Nathans J (1999) A new secreted protein that binds to Wnt proteins and inhibits their activities. Nature 398:431-436.

Huber AH, Nelson WJ, Weis WI (1997) Three-dimensional structure of the armadillo repeat region of beta-catenin. Cell 90:871-882.

Huber O, Korn R, McLaughlin J, Ohsugi M, Herrmann BG, Kemler R (1996) Nuclear localization of beta-catenin by interaction with transcription factor LEF-1. Mech Dev 59:3-10.

Ikeda S, Kishida S, Yamamoto H, Murai H, Koyama S, Kikuchi A (1998) Axin, a negative regulator of the Wnt signaling pathway, forms a complex with GSK-3beta and beta-catenin and promotes GSK-3beta-dependent phosphorylation of beta-catenin. EMBO J 17:1371-1384.

Inestrosa N, De Ferrari GV, Garrido JL, Alvarez A, Olivares GH, Barría MI, Bronfman M, Chacón MA (2002) Wnt signaling involvement in beta-amyloid-dependent neurodegeneration. Neurochem Int 41:341-344.

Inestrosa NC, Varela-Nallar L (2015) Wnt signalling in neuronal differentiation and development. Cell Tissue Res 359:215-223.

Jacque CM, Vinner C, Kujas M, Raoul M, Racadot J, Baumann NA (1978) Determination of glial fibrillary acidic protein (GFAP) in human brain tumors. J Neurol Sci 35:147-155.

Janeckova L, Fafilek B, Krausova M, Horazna M, Vojtechova M, Alberich-Jorda M, Sloncova E, Galuskova K, Sedlacek R, Anderova M, Korinek V (2016) Wnt Signaling Inhibition Deprives Small Intestinal Stem Cells of Clonogenic Capacity. Genesis 54:101-114.

Jelitai M, Anderová M, Chvátal A, Madarász E (2007) Electrophysiological characterization of neural stem/progenitor cells during in vitro differentiation: study with an immortalized neuroectodermal cell line. J Neurosci Res 85:1606-1617.

Kaneko N, Sawamoto K (2009) Adult neurogenesis and its alteration under pathological conditions. Neurosci Res 63:155-164.

Karalay O, Doberauer K, Vadodaria KC, Knobloch M, Berti L, Miquelajauregui A, Schwark M, Jagasia R, Taketo MM, Tarabykin V, Lie DC, Jessberger S (2011) Prospero-related homeobox 1 gene (Prox1) is regulated by canonical Wnt signaling and has a stage-specific role in adult hippocampal neurogenesis. Proc Natl Acad Sci U S A 108:5807-5812.

Kasantikul V, Shuangshoti S (1989) Positivity to glial fibrillary acidic protein in bone, cartilage, and chordoma. J Surg Oncol 41:22-26.

Katsumoto T, Mitsushima A, Kurimura T (1990) The role of the vimentin intermediate filaments in rat 3Y1 cells elucidated by immunoelectron microscopy and computer-graphic reconstruction. Biol Cell 68:139-146.

Kunke D, Bryja V, Mygland L, Arenas E, Krauss S (2009) Inhibition of canonical Wnt signaling promotes gliogenesis in P0-NSCs. Biochem Biophys Res Commun 386:628-633.

Kuwabara T, Hsieh J, Muotri A, Yeo G, Warashina M, Lie DC, Moore L, Nakashima K, Asashima M, Gage FH (2009) Wnt-mediated activation of NeuroD1 and retro-elements during adult neurogenesis. Nat Neurosci 12:1097-1105.

Kühl M, Sheldahl LC, Malbon CC, Moon RT (2000) Ca2+/calmodulin-dependent protein kinase II is stimulated by Wnt and Frizzled homologs and promotes ventral cell fates in Xenopus. Journal of Biological Chemistry 275:12701-12711.

Lavado A, Lagutin OV, Chow LM, Baker SJ, Oliver G (2010) Prox1 is required for granule cell maturation and intermediate progenitor maintenance during brain neurogenesis. PLoS Biol 8.

Li L, Hutchins BI, Kalil K (2009) Wnt5a induces simultaneous cortical axon outgrowth and repulsive axon guidance through distinct signaling mechanisms. J Neurosci 29:5873-5883.

Lie DC, Colamarino SA, Song HJ, Désiré L, Mira H, Consiglio A, Lein ES, Jessberger S, Lansford H, Dearie AR, Gage FH (2005) Wnt signalling regulates adult hippocampal neurogenesis. Nature 437:1370-1375.

Lin SC, Bergles DE (2002) Physiological characteristics of NG2-expressing glial cells. J Neurocytol 31:537-549.

Liu C, Li Y, Semenov M, Han C, Baeg GH, Tan Y, Zhang Z, Lin X, He X (2002) Control of beta-catenin phosphorylation/degradation by a dual-kinase mechanism. Cell 108:837-847.

Merkle FT, Mirzadeh Z, Alvarez-Buylla A (2007) Mosaic organization of neural stem cells in the adult brain. Science 317:381-384.

Mirzadeh Z, Merkle FT, Soriano-Navarro M, Garcia-Verdugo JM, Alvarez-Buylla A (2008) Neural stem cells confer unique pinwheel architecture to the ventricular surface in neurogenic regions of the adult brain. Cell Stem Cell 3:265-278.

Misra K, Mishra K, Gui H, Matise MP (2008) Prox1 regulates a transitory state for interneuron neurogenesis in the spinal cord. Dev Dyn 237:393-402.

Misson JP, Edwards MA, Yamamoto M, Caviness VS (1988) Mitotic cycling of radial glial cells of the fetal murine cerebral wall: a combined autoradiographic and immunohistochemical study. Brain Res 466:183-190.

Miyata T, Maeda T, Lee JE (1999) NeuroD is required for differentiation of the granule cells in the cerebellum and hippocampus. Genes Dev 13:1647-1652.

Miyata T, Kawaguchi A, Okano H, Ogawa M (2001) Asymmetric inheritance of radial glial fibers by cortical neurons. Neuron 31:727-741.

Mosimann C, Hausmann G, Basler K (2009) Beta-catenin hits chromatin: regulation of Wnt target gene activation. Nat Rev Mol Cell Biol 10:276-286.

Muotri AR, Chu VT, Marchetto MC, Deng W, Moran JV, Gage FH (2005) Somatic mosaicism in neuronal precursor cells mediated by L1 retrotransposition. Nature 435:903-910.

Nichols NR, Day JR, Laping NJ, Johnson SA, Finch CE (1993) GFAP mRNA increases with age in rat and human brain. Neurobiol Aging 14:421-429.

Nishiyama A, Dahlin KJ, Prince JT, Johnstone SR, Stallcup WB (1991) The primary structure of NG2, a novel membrane-spanning proteoglycan. J Cell Biol 114:359-371.

Noctor SC, Martínez-Cerdeño V, Ivic L, Kriegstein AR (2004) Cortical neurons arise in symmetric and asymmetric division zones and migrate through specific phases. Nat Neurosci 7:136-144.

Ozawa M, Baribault H, Kemler R (1989) The cytoplasmic domain of the cell adhesion molecule uvomorulin associates with three independent proteins structurally related in different species. EMBO J 8:1711-1717.

Prajerova I, Honsa P, Chvatal A, Anderova M (2010) Distinct effects of sonic hedgehog and Wnt-7a on differentiation of neonatal neural stem/progenitor cells in vitro. Neuroscience 171:693-711.

Rakic P (1972) Mode of cell migration to the superficial layers of fetal monkey neocortex. J Comp Neurol 145:61-83.

Ransom BR, Sontheimer H (1992) The neurophysiology of glial cells. J Clin Neurophysiol 9:224-251.

Rapraeger A, Jalkanen M, Bernfield M (1986) Cell surface proteoglycan associates with the cytoskeleton at the basolateral cell surface of mouse mammary epithelial cells. J Cell Biol 103:2683-2696.

Rodriguez J, Esteve P, Weinl C, Ruiz JM, Fermin Y, Trousse F, Dwivedy A, Holt C, Bovolenta P (2005) SFRP1 regulates the growth of retinal ganglion cell axons through the Fz2 receptor. Nat Neurosci 8:1301-1309.

Roessmann U, Velasco ME, Sindely SD, Gambetti P (1980) Glial fibrillary acidic protein (GFAP) in ependymal cells during development. An immunocytochemical study. Brain Res 200:13-21.

Rosso SB, Inestrosa NC (2013) WNT signaling in neuronal maturation and synaptogenesis. Front Cell Neurosci 7:103.

Rosso SB, Sussman D, Wynshaw-Boris A, Salinas PC (2005) Wnt signaling through Dishevelled, Rac and JNK regulates dendritic development. Nat Neurosci 8:34-42.

Rowitch DH, Kriegstein AR (2010) Developmental genetics of vertebrate glial-cell specification. Nature 468:214-222.

Sakakibara S, Imai T, Hamaguchi K, Okabe M, Aruga J, Nakajima K, Yasutomi D, Nagata T, Kurihara Y, Uesugi S, Miyata T, Ogawa M, Mikoshiba K, Okano H (1996) Mouse-Musashi-1, a neural RNA-binding protein highly enriched in the mammalian CNS stem cell. Dev Biol 176:230-242.

Sancho-Tello M, Vallés S, Montoliu C, Renau-Piqueras J, Guerri C (1995) Developmental pattern of GFAP and vimentin gene expression in rat brain and in radial glial cultures. Glia 15:157-166.

Sawamoto K, Wichterle H, Gonzalez-Perez O, Cholfin JA, Yamada M, Spassky N, Murcia NS, Garcia-Verdugo JM, Marin O, Rubenstein JL, Tessier-Lavigne M, Okano H,

Alvarez-Buylla A (2006) New neurons follow the flow of cerebrospinal fluid in the adult brain. Science 311:629-632.

Seri B, García-Verdugo JM, McEwen BS, Alvarez-Buylla A (2001) Astrocytes give rise to new neurons in the adult mammalian hippocampus. J Neurosci 21:7153-7160.

Seri B, García-Verdugo JM, Collado-Morente L, McEwen BS, Alvarez-Buylla A (2004) Cell types, lineage, and architecture of the germinal zone in the adult dentate gyrus. J Comp Neurol 478:359-378.

Shafit-Zagardo B, Kalcheva N (1998) Making sense of the multiple MAP-2 transcripts and their role in the neuron. Mol Neurobiol 16:149-162.

Singer SJ, Nicolson GL (1972) The fluid mosaic model of the structure of cell membranes. Science 175:720-731.

Slater PG, Ramirez VT, Gonzalez-Billault C, Varela-Nallar L, Inestrosa NC (2013) Frizzled-5 receptor is involved in neuronal polarity and morphogenesis of hippocampal neurons. PLoS One 8:e78892.

Stallcup WB, Beasley L (1987) Bipotential glial precursor cells of the optic nerve express the NG2 proteoglycan. J Neurosci 7:2737-2744.

Städeli R, Hoffmans R, Basler K (2006) Transcription under the control of nuclear Arm/beta-catenin. Curr Biol 16:R378-385.

Suh H, Consiglio A, Ray J, Sawai T, D'Amour KA, Gage FH (2007) In vivo fate analysis reveals the multipotent and self-renewal capacities of Sox2+ neural stem cells in the adult hippocampus. Cell Stem Cell 1:515-528.

Tago K, Nakamura T, Nishita M, Hyodo J, Nagai S, Murata Y, Adachi S, Ohwada S, Morishita Y, Shibuya H, Akiyama T (2000) Inhibition of Wnt signaling by ICAT, a novel beta-catenin-interacting protein. Genes Dev 14:1741-1749.

Tashiro A, Sandler VM, Toni N, Zhao C, Gage FH (2006) NMDA-receptor-mediated, cell-specific integration of new neurons in adult dentate gyrus. Nature 442:929-933.

Taylor CR, Burns J (1974) The demonstration of plasma cells and other immunoglobulin-containing cells in formalin-fixed, paraffin-embedded tissues using peroxidase-labelled antibody. J Clin Pathol 27:14-20.

Tu J, Yang F, Wan J, Liu Y, Zhang J, Wu B, Zeng S, Wang L (2014) Light-controlled astrocytes promote human mesenchymal stem cells toward neuronal differentiation and improve the neurological deficit in stroke rats. Glia 62:106-121.

Varela-Nallar L, Inestrosa NC (2013) Wnt signaling in the regulation of adult hippocampal neurogenesis. Front Cell Neurosci 7:100.

Ventura A, Kirsch DG, McLaughlin ME, Tuveson DA, Grimm J, Lintault L, Newman J, Reczek EE, Weissleder R, Jacks T (2007) Restoration of p53 function leads to tumour regression in vivo. Nature 445:661-665.

von Koskull H (1984) Rapid identification of glial cells in human amniotic fluid with indirect immunofluorescence. Acta Cytol 28:393-400.

Wang DD, Krueger DD, Bordey A (2003) Biophysical properties and ionic signature of neuronal progenitors of the postnatal subventricular zone in situ. J Neurophysiol 90:2291-2302.

Wigle JT, Oliver G (1999) Prox1 function is required for the development of the murine lymphatic system. Cell 98:769-778.

Wigle JT, Chowdhury K, Gruss P, Oliver G (1999) Prox1 function is crucial for mouse lens-fibre elongation. Nat Genet 21:318-322.

Wu X, Tu X, Joeng KS, Hilton MJ, Williams DA, Long F (2008) Rac1 activation controls nuclear localization of beta-catenin during canonical Wnt signaling. Cell 133:340-353.

Yamagata M, Suzuki S, Akiyama SK, Yamada KM, Kimata K (1989) Regulation of cell-substrate adhesion by proteoglycans immobilized on extracellular substrates. J Biol Chem 264:8012-8018.

Yamaguchi Y, Ruoslahti E (1988) Expression of human proteoglycan in Chinese hamster ovary cells inhibits cell proliferation. Nature 336:244-246.

Yamasaki M, Yamada K, Furuya S, Mitoma J, Hirabayashi Y, Watanabe M (2001) 3-Phosphoglycerate dehydrogenase, a key enzyme for l-serine biosynthesis, is preferentially expressed in the radial glia/astrocyte lineage and olfactory ensheathing glia in the mouse brain. J Neurosci 21:7691-7704.

Yu X, Malenka RC (2003) Beta-catenin is critical for dendritic morphogenesis. Nat Neurosci 6:1169-1177.

8 ATTACHMENTS

Wnt signaling promotes neonatal neural stem/progenitor cells differentiation into cells with neuronal characteristics

Kriska Jan[1,2], Honsa Pavel[1], Dzamba David[1,2], Butenko Olena[1], Kolenicova Denisa[1], Tumova Lucie[1,3], Nahacka Zuzana[4], Andera Ladislav[4], Korinek Vladimir[1,3], Anderova Miroslava[1,2]

[1]Department of Cellular Neurophysiology, Institute of Experimental Medicine, Academy of Sciences of the Czech Republic, Prague, Czech Republic
[2]2nd Faculty of Medicine, Charles University, Prague, Czech Republic
[3]Laboratory of Cell and Developmental Biology, Institute of Molecular Genetics, Academy of Sciences of the Czech Republic, Prague, Czech Republic
[4]Laboratory of Cell Signalling and Apoptosis, Institute of Molecular Genetics, Academy of Sciences of the Czech Republic, Prague, Czech Republic

INTRODUCTION

The canonical Wnt signaling pathway has an important role in the embryonic development and establishment of neurogenic niches. Here we aimed to assess the effect of Wnt signaling on the differentiation potential of neural stem/progenitor cells (NS/PCs), isolated from the frontal lobe of the neonatal mouse brain, *in vitro*.

SUMMARY

Changes in the cell incidence, protein expression and electrophysiological properties, measured *in vitro*, indicate that the Wnt/β-catenin signaling pathway promotes neonatal NS/PCs differentiation into the cells with neuronal characteristics.

RESULTS

Three distinct current patterns among differentiated NS/PCs

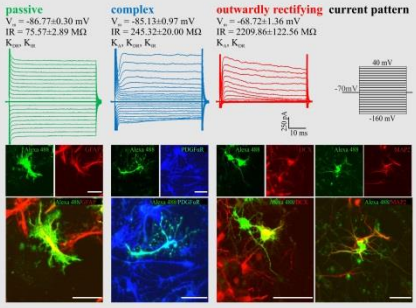

V_m - membrane potential; IR - input resistance; K_A - fast activating outwardly rectifying K^+ current; K_{DR} - delayed outwardly rectifying K^+ current; K_{IR} - inwardly rectifying K^+ current; GFAP - glial fibrillary acidic protein; PDGFαR - platelet-derived growth factor alpha receptor; DCX - doublecortin; MAP2 - microtubule-associated protein 2; scale bar 50 μm

Incidence of differentiated NS/PCs

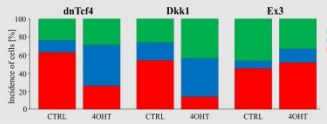

CTRL - control; 4OHT - 4-hydroxytamoxifen-treated cells

Voltage-gated Na^+ channels in $DCX^+/MAP2^+$ cells

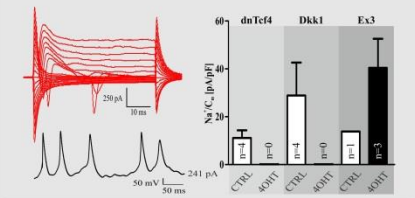

C_m - membrane capacitance; CTRL - control; 4OHT - 4-hydroxytamoxifen-treated cells; DCX - doublecortin; MAP2 - microtubule-associated protein 2; n - number of cells

Immunochemical analysis of NS/PCs

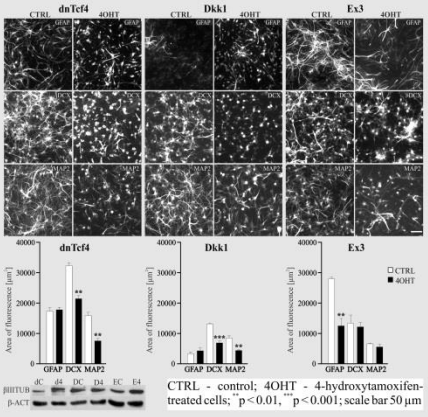

CTRL - control; 4OHT - 4-hydroxytamoxifen-treated cells; $^{**}p<0.01$, $^{***}p<0.001$; scale bar 50 μm

Voltage-gated K^+ channels in NS/PCs

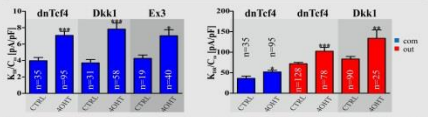

K_{IR} - inwardly rectifying K^+ current; K_{DR} - delayed outwardly rectifying K^+ current; C_m - membrane capacitance; n - number of cells; CTRL - control; 4OHT - 4-hydroxytamoxifen-treated cells; $^{*}p<0.05$, $^{**}p<0.01$, $^{***}p<0.001$

Ca^{2+} responses to glutamate/ATP application in $DCX^+/MAP2^+$ cells

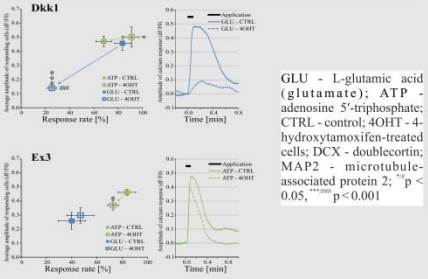

GLU - L-glutamic acid (glutamate); ATP - adenosine 5′-triphosphate; CTRL - control; 4OHT - 4-hydroxytamoxifen-treated cells; DCX - doublecortin; MAP2 - microtubule-associated protein 2; $^{**}p<0.05$, $^{***}p<0.001$

REFERENCES

Nusse R(2005)Cell Res. 15(1):28-32; **Prajerova I** et al.(2010)Neuroscience. 171(3):693-711; **Korinek V** et al.(1997)Science. 275(5307):1784-7; **Wu X** et al.(2008)Cell. 133(2):340-53; **Harada N** et al.(1999)EMBO J. 18(21):5931-42; **Ventura A** et al.(2007)Nature. 445(7128):661-5

SUPPORT

This project was supported by the grants GACR P303/12/0855, P304/12/G069 and GAUK 26214.

MATERIALS AND METHODS

Transgenic mouse strains

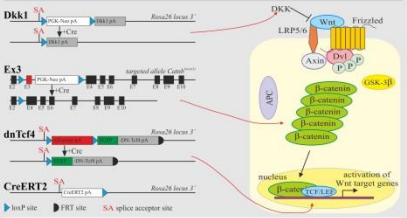

Cre - Cre recombinase; E2-E10 - exons; EGFP - enhanced green fluorescent protein; DKK - Dickkopf; LRP5/6 - Low-density lipoprotein 5/6; Dvl - Dishevelled; P - phosphorylation; APC - Adenomatous polyposis coli; GSK-3β - Glycogen synthase kinase 3β; TCF/LEF - T-cell factor/Lymphoid enhancer factor

β-catenin level in differentiated NS/PCs

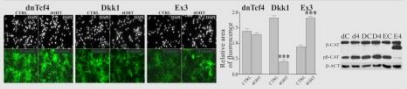

CTRL or C - control; 4OHT or 4 - 4-hydroxytamoxifen-treated cells; d - dnTcf4; D - Dkk1; E - Ex3; β-CAT - β-catenin; pβ-CAT - phosphorylated β-catenin; β-ACT - β-actin; $^{***}p<0.001$

Mouse strains: neonatal mice (P0-2); *Rosa26-tdTomato-EGFP/dnTCF4* and *Rosa26-Dkk1* as well as a mouse with targeted allele *Catnb-lox*^{Ex3} crossbred with a universal Cre deletor *Rosa26-creERT2*, enabling either the inhibition of Wnt signaling at the nuclear (*Rosa26*$^{nTCF4/creERT2}$; further termed dnTcf4) or membrane level (*Rosa26*$^{DKK1/creERT2}$; Dkk1) or its activation in the cytoplasm (*Catnb*$^{del(Ex3)/+}$*Rosa26*^{creERT2}; Ex3); Wnt signaling manipulation using 4-hydroxytamoxifen (4OHT; 1 μM) in the differentiation medium; 4OHT-untreated cells used as controls

Cell culture: cultured as neurospheres; maintained in Neurobasal-A medium supplemented with B-27, 2 mM glutamine, 1% penicillin/streptomycin/amphotericin (basal medium) and growth factors bFGF (10 ng/ml) and EGF (20 ng/ml) at 37 °C and 5% CO_2

Induction of differentiation: cells trypsinized and plated on PLL-coated coverslips at a cell density of $6x10^4/cm^2$ and treated with basal medium containing 20 ng/ml bFGF only; untreated (CTRL) and 4OHT-treated cultures

Electrophysiology: patch-clamp technique in the whole-cell configuration; cell membrane clamped from the holding potential of -70 mV to values ranging from -160 mV to 40 mV at intervals of 10 mV; pulse duration 50 ms

Immunocytochemistry: cell identification with antibodies against glial fibrillary acidic protein (GFAP), platelet-derived growth factor alpha receptor (PDGFαR), doublecortin (DCX) and microtubule-associated protein 2 (MAP-2)

Calcium imaging measurements: incubation in 4.5 μM OGB-1 AM and 0.09% Pluronic F-127 at 37°C; application of adenosine 5′-triphosphate (ATP) and L-glutamic acid (glutamate); fluorescence intensity (F) measured in the cell bodies; threshold for Ca^{2+} responses was 110% of the baseline fluorescence, and maximum intensity which occurred within 1 minute from the onset of application was taken into account

Western blot: lysis in 1x RIPA buffer with proteases and phosphatases inhibitors; total protein content determined by the Pierce BCA™ protein assay kit; SDS PAGE (10 – 15%); nitrocellulose membrane; detection with horseradish peroxidase

Data analysis and statistics: Data are presented as means ± S.E.M. (standard error of the mean) for n cells. Student's unpaired t-test was used to determine significant differences between the experimental groups. Values of $^{*}p<0.05$ were considered significant, $^{**}p<0.01$ very significant and $^{***}p<0.001$ extremely significant.

Figure 29: Poster from the 10th Conference of the Czech Neuroscience Society (Praha).